(Received 8 November 2025, Accepted 10 December 2025, Scheduled 5 January 2026)

Progress in Structured Light with Nonlinear Optics

Sachleen Singh and Andrew Forbes*

School of Physics, University of the Witwatersrand, Private Bag 3, Wits 2050, South Africa

ABSTRACT: The control of all of light's degrees of freedom and its harnessing for applications is captured by the emergent field of structured light. The modern toolkit includes external modulation of light with devices such as metasurfaces and spatial light modulators, their intra-cavity insertion for structured light directly at the source, and their deployment to engineer quantum structured light at the single photon and entangled state regimes. Historically, this control has involved linear optical elements, with nonlinear optics only recently coming to the fore. This has opened unprecedented functionality while revealing new paradigms for nonlinear optics beyond plane waves. In this review, we look at the recent progress in structured light with nonlinear optics, covering the fundamentals and the powerful applications they are facilitating in both the classical and quantum domains.

1. INTRODUCTION

Structured light [1] with linear optics elements is now common-place, allowing control of multi-dimensional and high-dimensional light in both space and time [2]. Recent trends have seen the emergence of a versatile digital toolkit [3], such as spatial light modulators and digital micro-mirror devices, modern design principles based on artificial atoms to build metasurfaces and metamaterials [4] as well as control of quantum states [5, 6]. Using this platform, new forms of light have emerged, allowing us to see smaller [7], focus tighter [8], communicate faster [9], and fuel new applications [10–12]. While nonlinearity is implicit in the design of structured light lasers [13], the structuring itself rarely depends directly on this. In bulk lasers, it is the deployment of intracavity linear elements that shapes the output, while on-chip structured light lasers have been largely restricted to orbital angular momentum and its derivatives, which can be achieved by a variety of symmetry breaking mechanisms [14].

Recently, nonlinear optics has been revisited in the context of structured light [15], offering a fresh perspective on nonlinear processes and their selection rules. This in turn has seen the emergence of a new toolkit with which to create, control and detect structured light, for what we term 'nonlinear structured light'. Nonlinear structured light offers not only a new toolkit but also a new way to addressing pressing challenges in the structured light community. For instance, accessing new wavelength regimes with structured light that would not otherwise be possible, e.g., through High-Harmonic Generation (HHG) and advancing ultrafast processes with structured light [16, 17], and moving structured light towards more extreme applications that demand high powers and intensities [18, 19]. At the other extreme, nonlinear rather than linear processes with quantum structured light are essential to overcome fundamental barriers [20], such as removing the need for ancillary photons in quantum networks, allowing interaction-free imaging at exotic wavelengths and facilitating novel sensors. In this review, we first cover the basics for the benefit of the reader before highlighting the recent progress in this field, from fundamentals to applications, from classical to quantum, and give our perspective on the future outlook.

1.1. Back to Basics

We observe a variety of light-matter interactions in daily life, such as diffused scattering from rough walls, reflection from water surfaces, and refraction through glass. These phenomena typically result from the *linear* optical response of materials, where the induced polarization P is proportional to the electric field E, following

$$P = \varepsilon_0 \chi^{(1)} E, \tag{1}$$

where ε_0 is the vacuum permittivity, and $\chi^{(1)} \approx 1$ is the linear susceptibility, and corresponds to electrons oscillating in an approximately harmonic potential. As the intensity of the incident light increases, the material response becomes nonlinear, making P a nonlinear function of the electric field,

$$P = \varepsilon_0 \left(\chi^{(1)} E + \chi^{(2)} E^2 + \chi^{(3)} E^3 + \cdots \right), \tag{2}$$

where $\chi^{(n)}$ are the nonlinear susceptibilities. These higher-order terms generate new frequency components resulting from anharmonic motion of bound electrons [21, 22]. Among these, the second-order nonlinearity ($n = 2$) is typically the most prominent, giving rise to effects such as second harmonic generation (SHG), although its magnitude is extremely small (e.g., $\chi^{(2)} \sim 10^{-12}$ m/V for quartz), making it difficult to observe at low light intensities.

In what follows we will outline the connection between structured light and nonlinear optics using second-order processes as an example, referring the reader to key texts to generalise the theory beyond this.

* Corresponding author: Andrew Forbes (andrew.forbes@wits.ac.za).

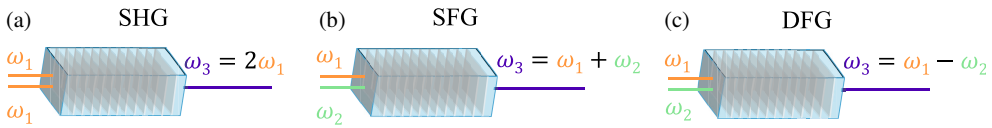

FIGURE 1. **Second-order nonlinear processes.** (a) Frequency doubling by a nonlinear crystal called second-harmonic generation (SHG). (b) The sum of input frequencies or sum frequency generation (SFG). (c) The difference of input frequencies or difference frequency generation (DFG).

1.2. Second-Order Nonlinear Optics

The second-order nonlinear processes are primarily governed by the quadratic polarization term, i.e.,

$$P(\omega_3) = \epsilon_o \chi^{(2)} E^2. \tag{3}$$

Say we have two input fields, E_1 and E_2, with different frequencies ω_1 and ω_2 incident on a nonlinear optical crystal. The resultant electric field can be written as a superposition of individual fields such as

$$E(t) = E_1 e^{-i\omega_1 t} + E_2 e^{-i\omega_2 t} + c.c.$$

The complex conjugate (c.c.) of each term is included to ensure that the resulting electric field E remains a real, physically meaningful quantity. After substitution for E in Eq. (3) we find,

$$P = \epsilon_o \chi^{(2)} \Big[\underbrace{E_1^2 e^{-2i\omega_1 t}}_{\text{I}} + \underbrace{E_2^2 e^{-2i\omega_2 t}}_{\text{II}} + \underbrace{2E_1 E_2 e^{-i(\omega_1+\omega_2)t}}_{\text{III}} + \underbrace{2E_1 E_2^* e^{-i(\omega_1-\omega_2)t}}_{\text{IV}} + c.c. \Big] + 2\epsilon_o \chi^{(2)} \underbrace{[E_1 E_1^* + E_2 E_2^*]}_{\text{V}}.$$

As illustrated in Fig. 1, terms I and II are responsible for second-harmonic generation, resulting in frequency doubling for ω_1 & ω_2 respectively [Fig. 1(a)]. Term III results in sum-frequency generation (SFG) where the output frequency is the sum of the input frequencies [Fig. 1(b)], while term IV gives rise to difference frequency generation (DFG), where the output frequency is the difference of the input frequencies [Fig. 1(c)]. Finally, optical rectification (which we will not consider here) is given by term V.

1.3. Phase-Matching

The efficiency of the second-order process is typically decided by the phase-matching between the polarization wave and the new frequency wave. Depending upon the NLC type (0, I, II) and the material, phase matching can be achieved using a variety of approaches [23, 24]. Since quasi-phase matching (QPM) is more efficient and allows all the waves to carry the same polarization, we present a phase matching example for this type based on periodically poled crystals, as shown in Fig. 2. A cartoon representation of the domains for a periodically poled crystal phase matched for DFG is shown in Fig. 2(a). Imagine two input laser beams to a crystal that produces DFG output, where all are polarized in the same direction. Since the medium refractive index varies with the wavelength, the phase velocities of the pump, signal, and DFG will differ from each other, resulting in a natural mismatch (Δk) among the momentum wavevectors such that $\Delta k = k_{\text{pump}} - k_{\text{signal}} - k_{\text{DFG}}$, as shown in Fig. 2(b). Physically, it introduces a phase difference between the polarization wave and DFG wave as they propagate along the crystal. This limits the gain in output intensity to a certain crystal length (ℓ_c) known as the coherence length, highlighted at the bottom of Fig. 2(c) for $\Delta k \neq 0$. To bring these waves back in phase, the sign of the nonlinear coefficient is flipped after every coherence length, shown as alternating stripes (each of opposite nonlinearity) [Fig. 2(d)], compensating the phase-mismatch with a crystal momentum vector (k_{crystal}). Since the sign of nonlinearity is the same for every two consecutive coherence lengths, the poling period (Λ) then becomes twice of ℓ_c, or in other words, $\Lambda = 2\ell_c$, which is typically of the order of micrometers depending upon the Sellmeir coefficients used [25]. Recently, the poling of domains of the order of 100 nm has been achieved, compensating for the largest phase-mismatch possible [26]. For perfect phase-matching, i.e., $\Delta k = 0$ as shown in Fig. 2(c), the rise in output intensity is exponential; however, the alteration of the sign of $\chi^{(2)}$ leads to a repetitive growth and decay of intensity when $\Delta k = k_{\text{crystal}}$.

1.4. Structured Light Through Second-Order Nonlinear Crystals

The nonlinear polarization wave term for DFG is proportional to the product of the input pump (E_1) and signal wave (E_2), such that

$$P(\omega_3) = \epsilon_o \chi^{(2)} E_1 E_2^*.$$

This suggests a product relationship between the complex amplitudes of the input beam structure [15]. For a paraxial nonlinear DFG system under no pump depletion and optimum phase matching, the expression for DFG wave E_3 and signal wave E_2 is given as

$$E_2 = E_2(0)\cosh \kappa z, \quad \kappa = \frac{\chi^{(2)} \omega_2 \omega_3 |E_1|}{\sqrt{k_2 k_3} c^2}$$

$$E_3 = i \left(\frac{n_2 \omega_3}{n_3 \omega_2} \right)^{1/2} \frac{E_1}{|E_1|} E_2^*(0) \sinh \kappa z,$$

where we assume that the source planes of the two input beams fall at the center of the nonlinear crystal, $z = 0$. Thus, at the interaction plane under the limit $z \to 0$ and using the approximation $\sinh \kappa z \approx \kappa z$, the equations become,

$$E_3 \approx i \left(\frac{n_2 \omega_3}{n_3 \omega_2} \right)^{1/2} \frac{E_1}{|E_1|} E_2^*(0) \left(\frac{\chi^{(2)} \omega_2 \omega_3 |E_1|}{\sqrt{k_2 k_3} c^2} \right) z,$$

and the complex amplitude E_3 at the crystal interaction plane can be simplified as,

$$E_3 \approx \eta E_1 E_2^*(0), \quad \eta = i \frac{\chi^{(2)} \omega_3}{n_3 c} z, \tag{4}$$

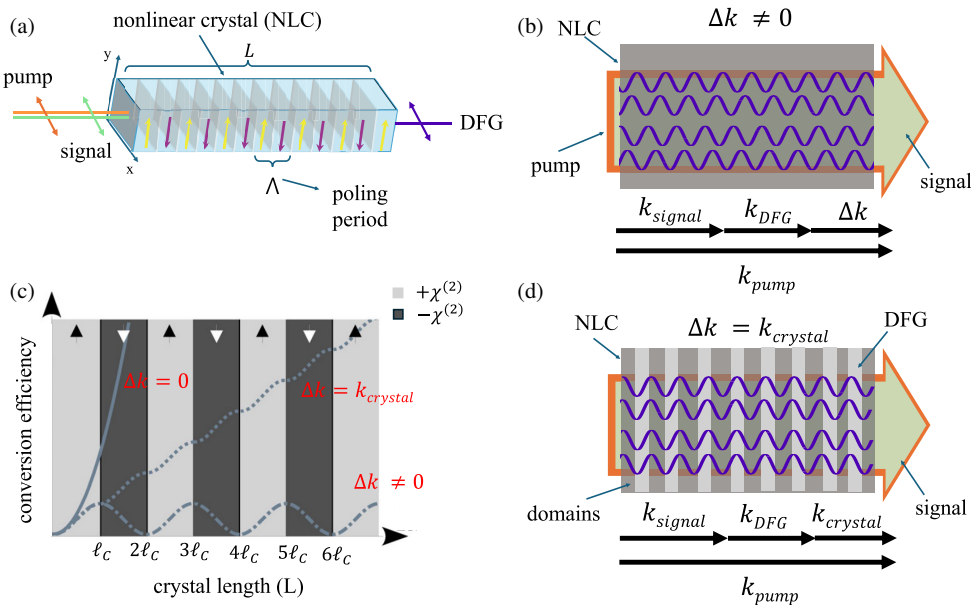

FIGURE 2. **Quasi-phase matching and periodic poling.** (a) A periodically poled nonlinear crystal (NLC) for type-0 collinear phase matching with poling period Λ generating an output beam (DFG) with a frequency of difference of input frequencies. (b) The phase-mismatched NLC with pump (k_{pump}) momentum vector equal to the sum of signal (k_{signal}), DFG (k_{DFG}) and phase mismatch-parameter Δk. (c) shows the conversion efficiency for ideal ($\Delta k = 0$), with quasi-phase matching ($\Delta k = k_{\text{crystal}}$), and without phase-matching ($\Delta k \neq 0$). (d) The structured crystal wave-vector k_{crystal} compensates for the phase mismatch among pump, signal, and DFG, resulting in higher conversion efficiency.

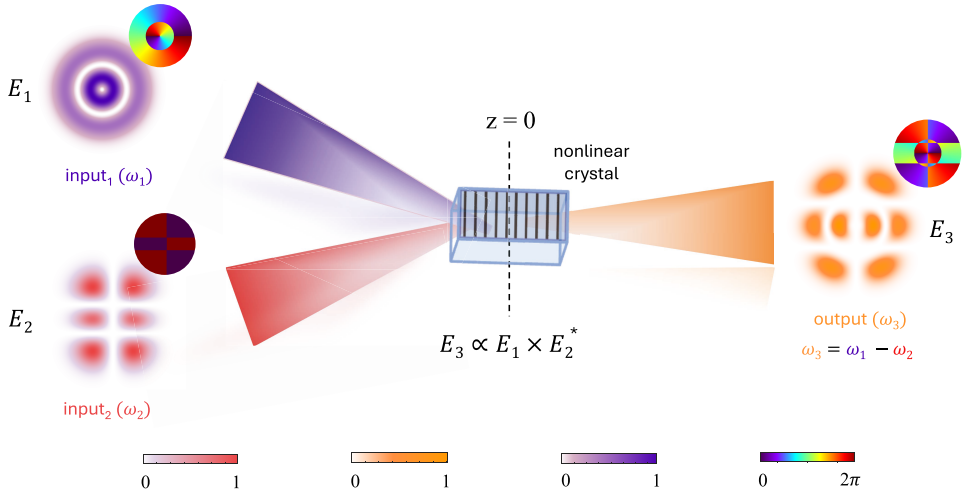

FIGURE 3. **Nonlinear control of spatial structure.** The new frequency beam is proportional to the product of input spatial modes, with each beam's source plane lying at $z = 0$. For DFG, the beam with a lower frequency undergoes phase conjugation upon frequency conversion, such that the output frequency is the difference of the input frequencies.

where $*$ represents the conjugate on the beam with the longer wavelength and η a function of physical constants including propagation distance, z. This relationship has been pictorially depicted in Fig. 3, where a Laguerre-Gauss (LG) mode at frequency ω_1 combines with an Hermite-Gauss (HG) mode at frequency ω_2 to generate a structured output mode at DFG frequency $\omega_1 - \omega_2$. Beyond the wavelength change, the output is a new mode that is the product of the two input electric fields. Since the product feature is common to SHG, SFG, and DFG, any second-order nonlinear process can be utilized to control light's structure [27]. Also, a similar expression to Eq. (4) has been obtained recently for stimPDC — a quantum analogue of DFG [28].

A good example of the product rule is for orbital angular momentum (OAM) structured light, such as Laguerre-Gauss, Bessel-Gauss, etc. Suppose each of the three modes (E_i) carries transverse amplitude $A_i(r)$ and phase $\phi_i(r)$, for $i = 1, 2, 3$. If two input wavelengths carry different topological charges, ℓ_1 and ℓ_2, for OAM of $\ell_1\hbar$ and $\ell_2\hbar$ per photon, respectively, it can be seen from Eq. (4) that real amplitudes multiply, and the complex phases subtract at the interaction plane,

$$A_3(r) = \eta A_1(r) A_2(r), \quad \phi_3(r) = \phi_1(r) - \phi_2(r),$$

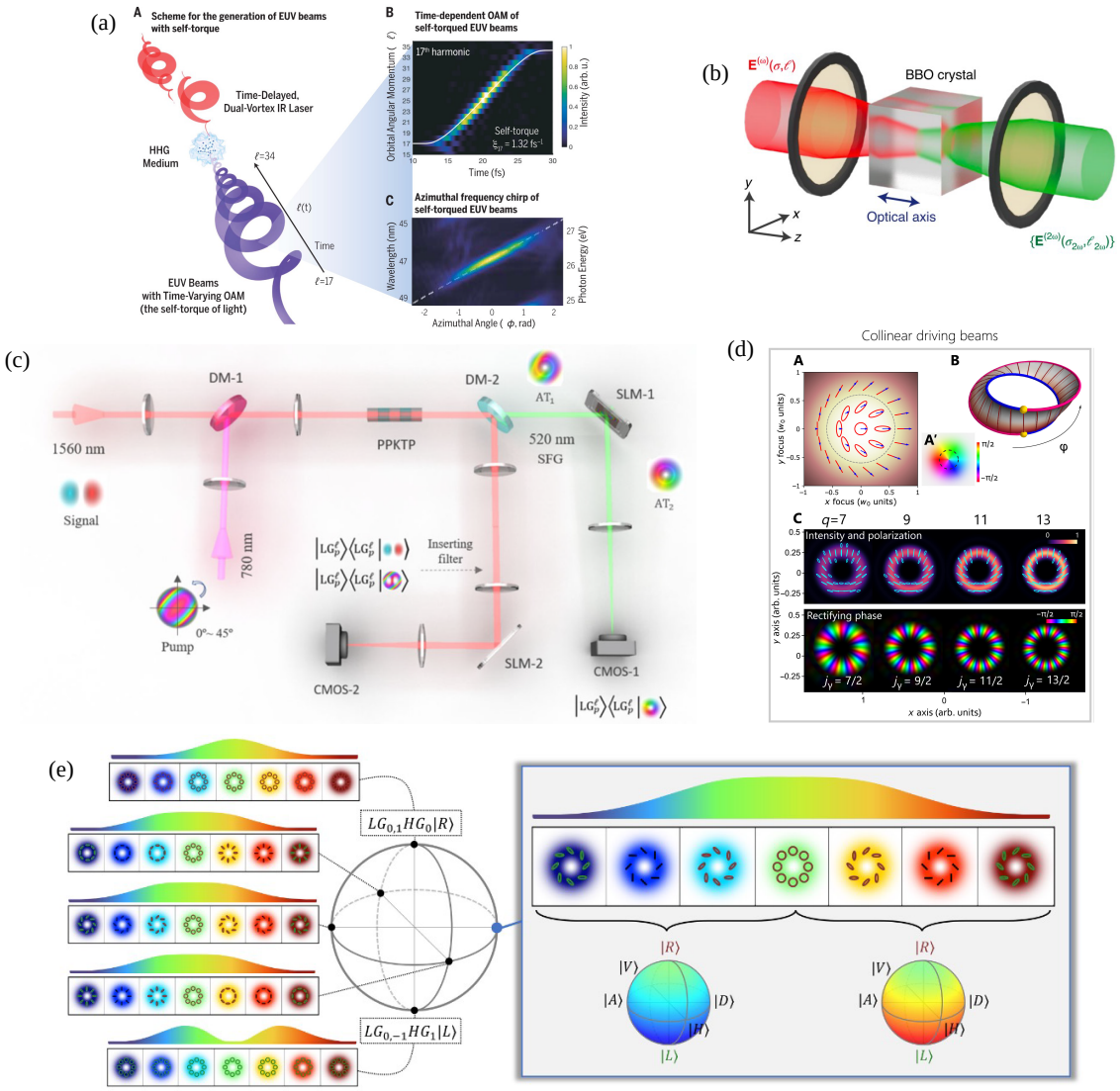

FIGURE 4. Nonlinear control for multiple degrees of freedom of structured light. (a) Two time-delayed pulses introduce a time-dependent nonlinear interaction, generating time varying orbital angular momentum (OAM) structured light. (b) When a nonlinear crystal interacts with a circularly polarized beam, it introduces spin-orbit coupling, which is further strengthened when the incoming beam is focused into the crystal. (c) New selection rules for frequency conversion of OAM (orbital angular momentum) structured light emerge when two input beams without net OAM interact nonlinearly to generate a new beam with a non-zero OAM. (d) But for upconversion of higher-order polarization topologies, isotropic nonlinearity is necessary, realizing the frequency conversion of both spin and OAM degrees of freedom of a Möbius strip. (e) Such spatial degrees of freedom (DoFs) can be combined with frequency, realizing spatio-spectral structured light represented on a multi-DoF Poincaré sphere. Figure reproduced with permission from: (a) Ref. [60], © AAAS; (b) Ref. [72], © Springer Nature Limited; (c) Ref. [75], © APS; (d) Ref. [78], © AAAS; (e) Ref. [58], © APS.

such that the nonlinear selection rule for OAM beams becomes [29]

$$\ell_3 = \ell_1 - \ell_2.$$

The output mode equal to the product of input modes is equally true for SFG under the limit $z \to 0$ [30], where $\sinh \kappa z$ is replaced by $\sin \kappa z$ [21]. The $z = 0$ can be an arbitrary plane at the NLC, meaning that the source plane of all three structured beams should overlap at the same position inside the NLC.

Equation (4) makes clear that the outcome from the process is the product of the structuring of the light (E_1 and E_2) and the medium, in this example, $\chi^{(2)}$. Structuring the former is possible through a wealth of tools (see Introduction), from cheap digital solutions to exotic metasurfaces, while the latter is possible through domain engineering [31], novel resonant [32] and structured [33, 34] matter. Of course, these approaches are not mutually exclusive [35], where combining the shaping functionalities opens the possibility for rewrittable nonlinearity with exciting future prospects [36, 37].

2. CLASSICAL NONLINEAR STRUCTURED LIGHT

Recently, nonlinear optics has emerged as a useful tool controlling various degrees of freedom (DoF) of structured light [15], be it individual shaping [38] or mixing amplitude [39], phase [40], polarization [41], time [42], wavelength

or frequency [43] together. This nonlinear control of light with light [44–47], has enabled new mechanisms to harness light's structure, initially demonstrated for OAM structured light three decades ago [48], now extended to vectorial light [49], quantum light [50] and multimode photonics [51]. A typical nonlinear extension to structured light is combining spatial DoFs with the wavelength or frequency via frequency conversion, be it for exploring new selection rules [52, 53] or changing the colour of structured light [54, 55], with a recent trend towards intermixing of DoFs whether to reveal new phenomenon [56, 57] or creating new forms of light [42, 58]. For instance, a time-dependent nonlinear interaction generates a time-varying orbital angular momentum when a non-perturbative high-harmonic process is driven by two pulses with a relative time delay, as depicted in Fig. 4(a). Ideally, for the qth harmonic order, two vortex beams with charges ℓ_1 and ℓ_2 should upconvert to OAM of $q\ell_1$ and $q\ell_2$ [59]. However, when a relative delay is introduced between the two pulses, the harmonic OAM is no longer restricted to discrete values, but instead evolves smoothly from $q\ell_1$ to $q\ell_2$, introducing self-torque of light. This continuous, time-dependent variation of orbital angular momentum can alternatively be viewed as if light is spiraling in time [60]. High-harmonic processes become accessible when the driving electric field reaches the strong-field regime, with amplitudes on the order of 0.1–1 V/Å, typically provided by few-cycle femtosecond pulses focused into noble gases such as Ar, Xe, or Kr [61]. More recently, this has been extended to air-lasing driven by a superfluorescence pump [62], introducing a cavity-free UV structured light source, albeit in a relatively bulky configuration. In contrast, combining a gain medium with a nonlinear crystal offers a more compact route to UV structured light via intracavity frequency doubling [63].

However, low-order nonlinear processes can be easily accessed with typical pump laser intensities (10^8 W cm^{-2}), realizing tunable structured light by pump shaping [64]. Further, by exploiting the birefringence of a nonlinear medium [65] or by tight focusing into the NLC [66], the polarization degree of freedom can be coupled with OAM DoF, whether to preserve it [67] or mix it with spatial DoFs [68]. For instance, in the linear regime, a crystal can act as a space-variant retarder producing spin-orbit coupled states at the fundamental frequency [69, 70]. These states are then upconverted through nonlinear processes, giving rise to multiple second-harmonic components with diverse spin-orbit content [71]. The propagation of the spin-orbit fields through the crystal strengthens the linear spin-orbit coupling before emerging as a cascade of nonlinear spin-orbit states as depicted in Fig. 4(b). By contrast, a collimated beam yielded only a single spin-orbit state following the typical OAM conservation selection rules [72]. Despite the change of frequency, the output beam OAM is equal to the sum [73] or difference of the input beams OAMs [74], a signature of parametric nonlinear processes. However, this may not seem to hold when an HG beam is upconverted with an astigmatic pump, as the new wavelength will carry an OAM mode while input modes carry none, as highlighted in Fig. 4(c). This anomaly has been attributed to the fact that the unconverted pump also carries a structure, which has not been accounted for the net OAM calculation [75]. It was observed that the lost OAM is hidden in the residual pump that maintains the OAM conservation. However, an anisotropic nonlinear medium, like an NLC, is not sufficient to preserve the polarization structure of the beam [76, 77]. Recently, an isotropic gaseous medium was used to demonstrate the conservation of generalized angular momentum (both spin and OAM) by driving high-harmonic generation with vector beams [78], realizing up-conversion of polarization topologies (Fig. 4(d)). Furthermore, such nonlinear control of spatial DoFs has recently been extended to the frequency domain by inducing a polarization-dependent temporal splitting of a laser pulse in a BBO crystal, which generates nonseparable states in space and frequency [58]. Subsequent spatial modulation of such states then gives rise to spatio-spectral Poincaré beams, introducing a multi-degree-of-freedom Poincaré sphere to represent light structured simultaneously in space, frequency, and polarization, as shown in Fig. 4(e).

Although we have predominantly focused on nonlinear processes as if they have little in common, recent work has revealed new mechanisms at play that brings these domains closer together, demonstrated with OAM modes in a FWM degenerated process in a Rb vapor cell [79]. The output could be understood as a two-channel three-wave mixing process, where the spatial structures for the output fields were simply the square of one input field times the conjugate of the other. Further, when one input was a Gaussian mode, the spatial structure of each conversion channel was equivalent to SHG and parametric downconversion for the other two fields. The situation becomes more intricate when polarization is added into the mix, as has been revealed using vectorial OAM light under FWM, also in an Rb vapor cell [80]. Multiple "pathways" for the FWM output appear due to the interaction of spin-orbit coupling between the light and the atomic system, enriched by the many Zeeman sublevels coupling with circularly polarized light components. Intriguingly, the explanation of the final output requires a quantum interference perspective, where the possible "pathways" interfere to produce the structured output. These works highlight how structured light opens new perspectives that not only enrich nonlinear processes, but also reveal the hidden connections yet to be unleashed, and exciting applications already appearing [81–83].

3. QUANTUM NONLINEAR STRUCTURED LIGHT

Quantum structured light [5, 6] is attractive for its large Hilbert space and tailoring the properties of the state itself. Nonlinear optics has a long history in the context of quantum light and indeed is the workhorse for the creation of entangled photons by spontaneous parametric downconversion (SPDC), where conservation is exploited for correlation. The functionality can be enhanced by shaping of the SPDC or FWM pump light, which in turn alters the spatial correlations of the output [84–86], as well as structuring both the light and the crystal [87] [Fig. 5(a)]. The SPDC crystals can be cascaded in user-defined paths to produce high-dimensional OAM entanglement [88] with correlations not restricted to the SPDC process itself [Fig. 5(b)]. Beyond natural nonlinear materials at the creation step, a mod-

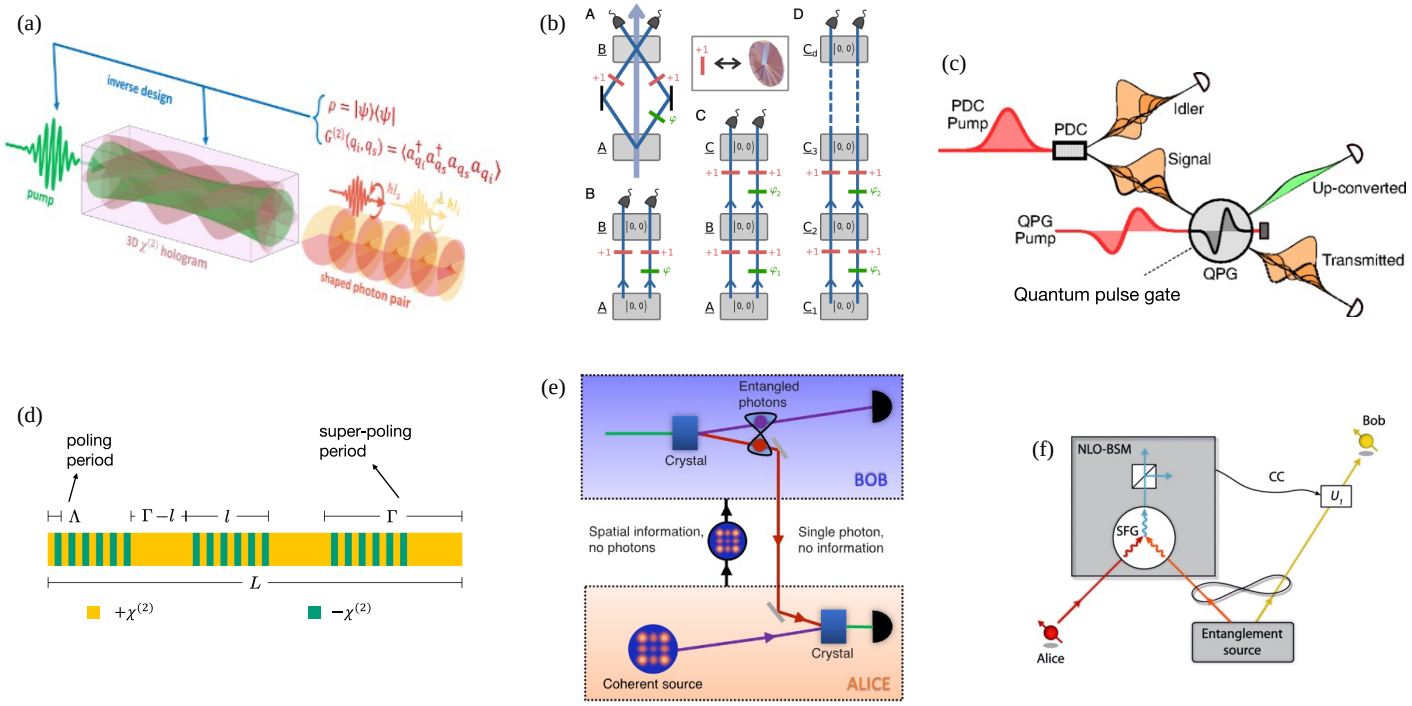

FIGURE 5. Quantum nonlinear optics. (a) Creation of entangled photons by structuring the crystal and the pump beams. (b) High-dimensional entanglement generation by path identity. (c) A quantum pulse gate, enabled by dispersion-engineered sum-frequency generation, for reconstructing high-dimensional quantum states. (d) A multi-output quantum pulse gate is developed by poling and super-poling of a $LiNbO_3$ waveguide. (e) One photon from an entangled pair is upconverted by another crystal, realizing a 15-dimensional quantum channel for spatial modes. (f) Sum frequency generation (SFG) based nonlinear Bell state analyzer for faithful quantum teleportation. Figure reproduced with permission from: (a) Ref. [87], © Optica; (b) Ref. [88], © PNAS; (c) Ref. [96], © APS; (d) Ref. [97], © APS; (e) Ref. [101], © Springer Nature; (f) Ref. [104], © APS.

ern trend is to engineer structured second-order nonlinearity in bulk [89] or using metamaterials [90], already used to structure the correlations in many DoFs. All these approaches allow for customised quantum light at the source.

Nonlinear optics also has an important role to play in the detection of quantum states, leveraging off the preservation of entanglement and coherence in nonlinear processes [91]. It has become a common use for efficient photon detection [92], particularly for measurement of telecom wavelength photons [93]. While a quantum state tomography (QST) is often done by linear projective measurements, dispersion-engineered sum-frequency generation can do the same in the time-frequency domain [94] using so-called quantum pulse gates [95]. This has allowed a $d = 7$ dimensional tomography [96] [Fig. 5(c)], recently extended to $d = 5$ dimensional deterministic projections [97, 98], the latter made possible by domain engineering the nonlinear crystal [Fig. 5(d)]. These time domain tools have also allowed for the efficient demultiplexing of temporal modes [99] and multiplexing by difference frequency generation [100].

Nonlinear optics can overcome a major obstacle to many high dimensional quantum protocols: the need for ancillary photons, whose number increases with dimension. These photons require ever more SPDC sources of entanglement, making the multiphoton detection step prohibitive. For this reason, the state of the art in teleportation remains at $d = 3$ dimensional states. Recent progress has seen sum frequency generation (SFG) used for spatial mode transport in $d = 15$ using OAM [101] (Fig. 5(e)), and image transport in the pixel basis [102]. Both these experiments used a SPDC crystal and two entangled photons as a quantum resource, with the information from a bright classical beam "teleported" to one of the single photons. While the experiments had all the hallmarks of teleportation, the need for a bright beam to overcome efficiency issues meant no entanglement swapping was involved, so far achieved only in polarization DoF [103]. True teleportation has recently been shown in $d = 3$ dimensions using time-bin states, facilitated by enhanced SFG efficiency in a nanophotonic cavity [104] (Fig. 5(f)).

4. APPLICATIONS

The control discussed in the prior sections has been harnessed for new applications. The concept of 2D nonlinear holography has emerged as a useful tool for controlling the transverse degrees of freedom of structured light both digitally [105] or by physically embedding a hologram into the crystal structure [106, 107] or in thin metasurfaces [33]. While thin metasurfaces provide a phase-matching free route to mix different degrees of freedom of structured light [108–111], bulk crystals allow generation of 3D structured light, by engineering ferroelectric-domains [112, 113]. By tailoring the $\chi^{(2)}$ profile, one can customize the output structure to carry the desired orbital angular momentum (OAM) and radial order directly from the NLC [112]; on the other hand, replacing the traditional striped poling with a dotted pattern improves the fidelity of the

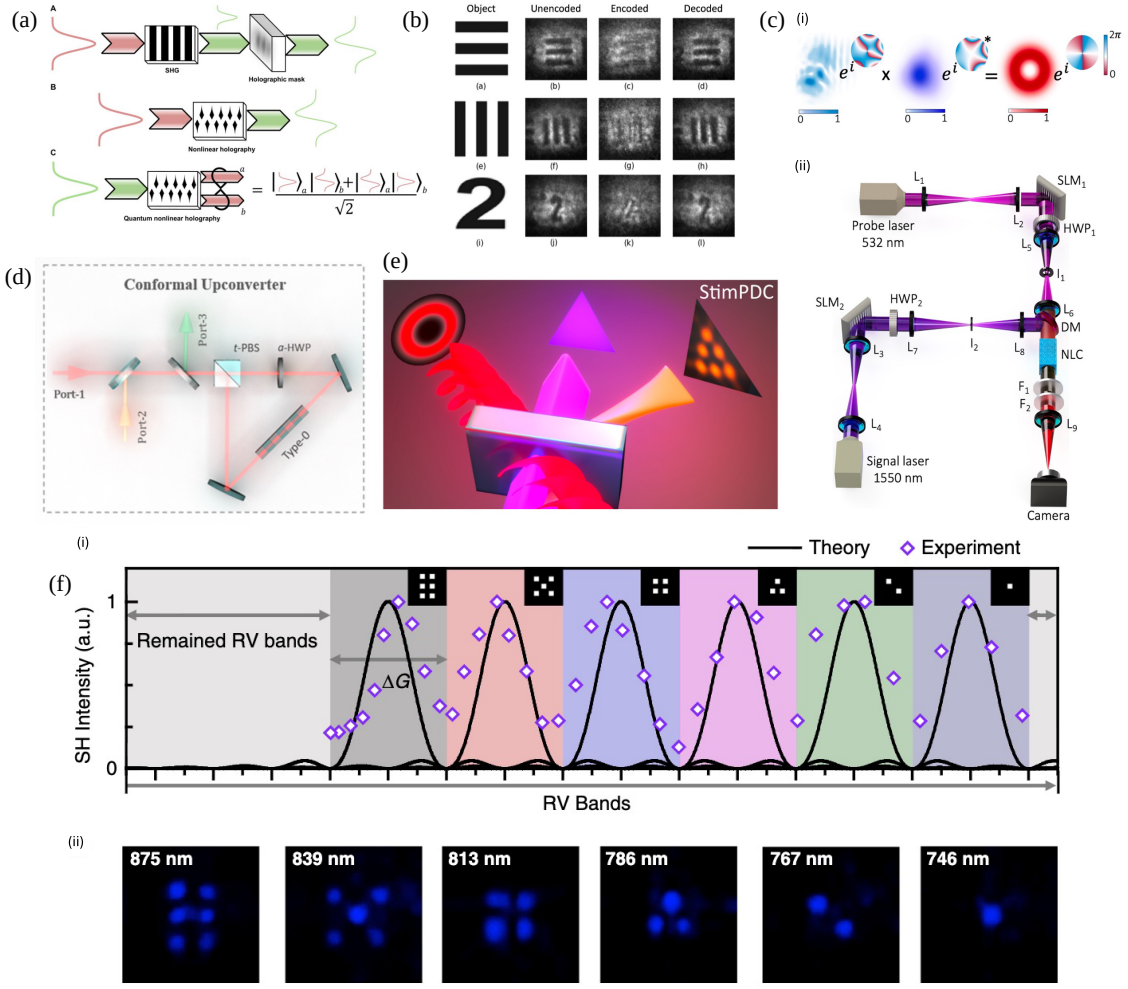

FIGURE 6. **Nonlinear structured light applications.** (a) Shaping all three dimensions of the nonlinear crystal (NLC) to structure the quantum correlations at the source is useful for quantum nonlinear holography. (b) With usual nonlinear holography, one can encode object information that can be decoded only when the correct phase is applied by a receiver, enabling orthogonal spatial encoding. (c) The measurement-free adaptive optics for structured light is achieved when the product and phase-conjugation features of difference frequency generation are combined, useful for adaptive optics applications. (d) The frequency conversion of vector beams can be utilized for generating versatile polarization patterns of vectorial structured light. (e) Two independent coherent sources can be combined nonlinearly, such that light can be made to diffract off light, a potential tool for orbital angular momentum detection. (f) Shaping the full 3D momentum space of the NLC allows multi-wavelength phase matching of the crystal, useful for optical storage applications. Figure reproduced with permission from: (a) Ref. [114], © AAAS; (b) Ref. [118], © Optica; (c) Ref. [120], © SPIE; (d) Ref. [129], © Optica; (e) Ref. [128], © Optica; (f) Ref. [132], © Springer Nature Limited.

structured-light generation at the new frequency [113]. This 3D control has been further extended to shape the quantum correlations at the source, with a minimal toolkit requiring only a structured crystal and a laser source [114], the resulting crystal structure is highlighted in Fig. 6(a). Furthermore, recently a structured light source generating EPR-like correlations, called a random hologram was introduced [115], where the role of the nonlinear kernel $\chi^{(2)}(\mathbf{r})E_p(\mathbf{r})$ in SPDC is effectively played by the squared pump field $E_p^2(\mathbf{r})$ inside the second-order correlation integral, replacing the need for inefficient nonlinear frequency conversion. These quantum-like correlations are then exploited to demonstrate nonlocal image recognition and sensitive phase metrology with bright classical light, emulating the functionality of a high-flux SPDC source [116].

While spontaneous parametric down conversion enables the generation of two photons out of a single photon [5], however, its reverse process, namely SFG, can be used to decode the photon information in the spectral degree of freedom [117]. Recently, its analog has been achieved in the spatial degree of freedom by encoding an image with a structured phase mask, which can only be recovered when a conjugate phase mask is used by the receiver [118]. The authors leveraged the natural phase conjugation provided by nonlinear DFG process to decode the image, which allows them to cancel the unwanted aberrations from the signal [Fig. 6(b)]. Furthermore, this natural wavefront reversal by coupling either light with sound [119] or light with light [120] has recently demonstrated for automatic turbulence mitigation in optical communications [121] and wavelength-adaptive modal decomposition with structured light [122], an example for OAM structured light has been highlighted in Fig. 6(c). This recent realization that nonlinear structured light can serve as an in-vivo guide star may

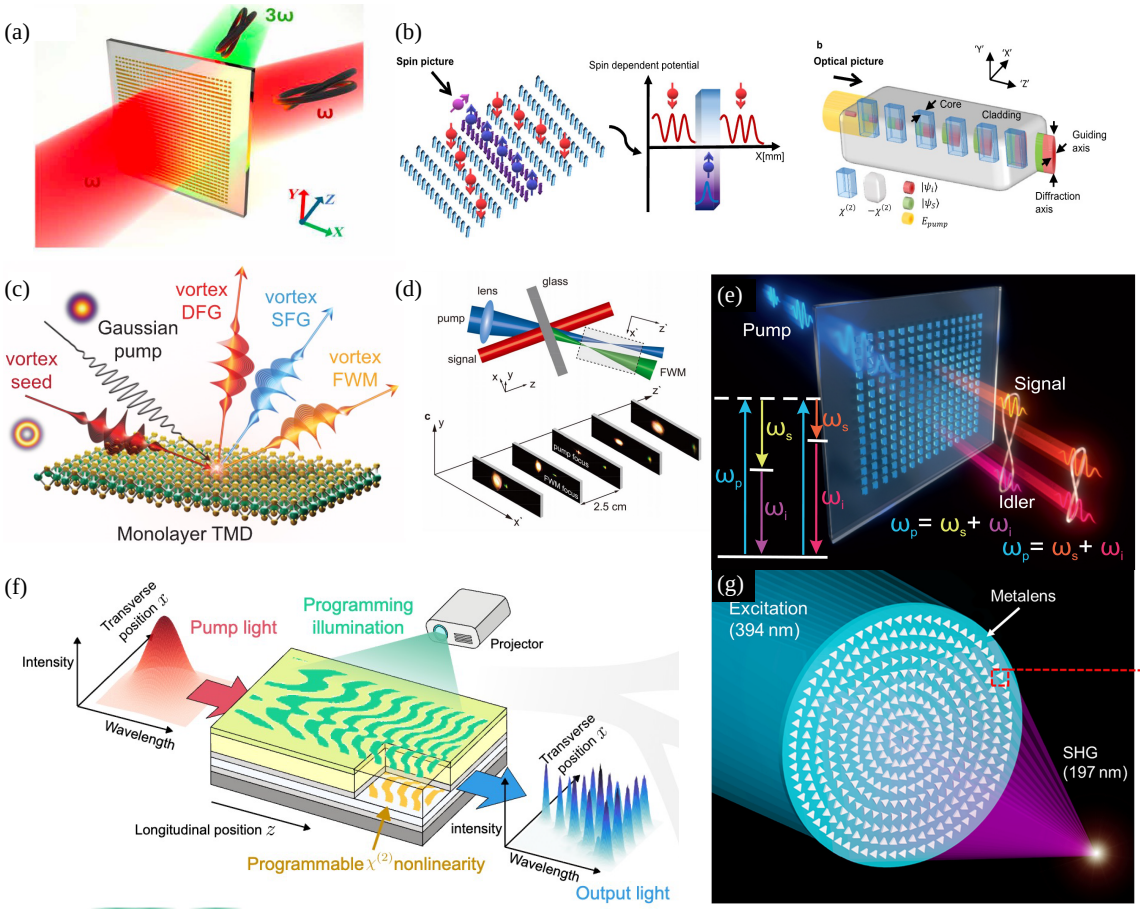

FIGURE 7. **Emerging platforms and applications of nonlinear structured light.** (a) Nonlinear holography is useful for imprinting holograms onto the meta-atoms themselves, allowing to encode topology both into the fundamental and the third harmonic generation. (b) The 3D structure of the nonlinear crystal (NLC) can be shaped to guide light within the NLC, emulating the spin-transport of electrons in magnetic materials. (c) Monolayer van der waals NLCs can be exploited to circumvent phase-matching, allowing both $\chi^{(2)}$ and $\chi^{(3)}$ processes within a single NLC. (d) Four-wave mixing with a simple planar glass slab can also be utilized to shape light useful for tuning the focal spot of the new beam. (e) Nonlinear metasurfaces are useful for broadband control of the quantum correlations, enabling efficient and tunable spontaneous parametric downconversion. (f) The $\chi^{(2)}$ domains can be programmed using structured illumination and can be updated in real time, allowing control over both spatial and spectral degrees of freedom of nonlinear structured light. (g) The subwavelength structure of nonlinear metasurfaces can be utilized for efficient second harmonic generation for very short UV wavelengths, which can be very useful for designing optical elements (lenses) for the deep-UV (< 200 nm) spectral regime. Figure reproduced with permission from: (a) Ref. [152], © AAAS; (b) Ref. [154], © Springer Nature Limited; (c) Ref. [156], © ACS; (d) Ref. [159], © Springer Nature Limited; (e) Ref. [161], © AAAS; (f) Ref. [37], © Springer Nature Limited; (g) Ref. [168], © AAAS.

be very useful for deep tissue imaging with fluoroscence microscopy [123, 124].

Most of the commonly used nonlinear crystals are birefringent, e.g., $LiNbO_3$, BBO, PPKTP, LBO, allowing easy switching of the polarization of the input mode and making them a useful potential tool for controlling the polarization degree of freedom [105, 125]. Now, depending upon the type of crystal, the orthogonal/same components of the input polarization mode will be multiplied to generate a new frequency mode [126, 127]. However, for spatially varying polarization patterns, such as in vector beams, the output polarization pattern will depend upon the type of crystal used [126, 128]. To preserve the polarization, one can introduce a type-0 NLC in a Sagnac geometry with a half-wave plate placed asymmetrically in the loop (Fig. 6(d)). This allowed the authors to preserve the vector beam polarization pattern through the frequency conversion, very useful for nonlinear applications in vectorial structured light [129].

In linear optics, two coherent sources of light add to generate a new structure; in contrast, nonlinear optics allows multiplication of two sources [27]. But with type-II SHG, a single source is enough for frequency conversion, where the signal structure gets multiplied by unmodulated Gaussian in orthogonal polarization, useful for applications with high-fidelity upconversion of structured light [105]. This multiplication of light with light allows the creation of new patterns of light, for example, light can be made to diffract off light using a virtual triangular object created entirely out of light, as depicted in Fig. 6(e), adding a new nonlinear tool for detecting OAM structured light [128].

Such nonlinear structuring of light can also be achieved by third-harmonic generation (THG). Recently, by exploiting the rotational symmetry of an isotropic Si metasurface, the to-

TABLE 1. Reported absolute conversion efficiencies (ratio of output harmonic power to pump power) for representative nonlinear crystals and metasurfaces at common pump wavelengths for SHG (unless otherwise specified). OPG — optical parametric generation. Bracketed numbers correspond to bibliography entries.

Pump → SHG $\omega \rightarrow 2\omega$ **(wavelength)**	**Nonlinear crystal material**	η **(abs.)**	**Nonlinear metasurface material**	η **(abs.)**
532 → 266 nm	CLBO/KDP	∼60% [169, 170]	ZnO	$\sim 10^{-8}$ [167, 168]
800–900 → 400–450 nm	BBO/BIBO	∼40% – ∼50% [171, 172]	$LiNbO_3$, GaAs, Au/ZnO	$\sim 10^{-3}$–10^{-6} [173–176]
1064 → 532 nm	KTP/LBO	>55% [177–179]	Ag	[180]
1550 → 775 nm	PPLN	∼70% (waveguide) [181]	$LiNbO_3$, AlGaAs	$\sim 10^{-8}$–10^{-3} [182–185]
2.4 µm (OPG)	$ZnGeP_2$	∼22% [186]	-	-

tal angular momentum selection rule $m_{3\omega} = 3m_{\omega}$ has been demonstrated. When a circularly polarized beam is tightly focused in a $\chi^{(3)}$ thin film, induces three spin-orbit coupled pump photons to combine into one third-harmonic photon, enforcing the nonlinear addition of non-paraxial light [130]. So far, we shave only discussed applications of 2D holography; however, the full structure of the crystal can be shaped to encode 3D holograms [131]. Recently, it has been utilized for multi-wavelength phase matching, enabling pattern creation in 6 different channels, as shown in Fig. 6(f), opening up new avenues for optical storage applications [132].

Moving away from synthetic crystals to biological processes, the extension of nonlinear structured light to natural nonlinear processes in biological samples is pushing the boundaries of nonlinear microscopy. Structured excitation beams such as Gaussian, Bessel and Airy profiles have been shown to tailor contrast and field of view in linear and nonlinear light-sheet and fluorescence microscopy, enabling fast volumetric two-photon tomography in complex tissues [133–135]. More generally, structured illumination microscopy (SIM) exploits patterned light to achieve super-resolution with high temporal bandwidth [136], and recent work combining adaptive optics, multifocal excitation, and nonlinear SIM has delivered deep-tissue super-resolution imaging with improved robustness to aberrations [137]. Recently, a new approach to achieve super-resolution SIM when combined with Raman microscopy, where instead of using conventional Moiré patterns, Lee et al. randomize the k-space using random distribution of gold nanoparicles, effectively achieving 2 times image resolution over the diffraction limit [138]. Parallel advances in NIR-II fluorescence and light-sheet platforms further enhance penetration depth and image contrast [139], while recent i^2PIE-compressed supercontinuum implementation exemplifies how optimal nonlinear pulse compression directly improves contrast in nonlinear light-sheet microscopy [140].

Spatial degrees of freedom have long been exploited for nonlinear imaging, beginning with photorefractive crystals, where two-wave mixing enabled early demonstrations of nonlinear image formation [141, 142]. This was later followed by three-wave mixing approaches, such as nonlinear negative refraction in thin BBO slices, which bend an infrared signal into a visible idler at a tunable negative angle and provide nonlinear focusing for enhanced image resolution [143]. With the advent of advanced holographic techniques, nonlinear structuring of light has expanded significantly, enabling improvements to the field of view [144] and increasing the information capacity of imaging systems through domain-engineered lithium-niobate nonlinear holograms [144, 145]. While material engineering offers powerful routes for integrated and on-chip applications, digital modulation tools provide complementary, highly dynamic control for biomedical imaging [146] and high-contrast image recognition [83]. These digital approaches naturally extend many linear imaging techniques, such as spiral phase contrast imaging, spiral interferometry, and spatial differential imaging, into the nonlinear regime. Most recently, by placing a spiral phase plate at the rear focal plane of an imaging system, nonlinear spiral-phase interferometry has been demonstrated, enabling high-contrast imaging of domain structures through nonlinear interference of spiral phase and point spread function [147].

5. EMERGING TRENDS

While NLCs excel in delivering higher conversion efficiencies, thin nonlinear metasurfaces are particularly attractive for reducing the footprint of integrated devices, since their thickness is on the order of the wavelength of light [148, 149]. However, their efficiency is limited by strong pump absorption loss as seen in chalcogenide metasurfaces [150]. Recently, this strong pump absorption is customized, achieving near-IR to mid-IR upconversion in an amorphous-Si metasurface by combining high-Q resonant pump with broadband FWM signal [151]. Furthermore, by engineering metasurfaces to operate within the pump's low absorption spectral band, the ability to encode and transfer the wavefront topology of the fundamental field has been demonstrated via a structured $\chi^{(3)}$ third-harmonic as shown in Fig. 7(a), while the $\chi^{(1)}$ linear response controlled by the same geometry simultaneously [152].

Though nonlinear metasurfaces are effective platforms for generating two-dimensional structured light [153], their efficiencies are typically lower than bulk crystals. To make this distinction quantitative, a side-by-side comparison of reported

SHG conversion efficiencies for commonly cited material platforms is presented at the end of this section (Table 1). By contrast, NLCs can exploit all spatial degrees of freedom, owing to their three-dimensional volume, opening opportunities beyond 2D shaping. This capability was recently demonstrated by Yesharim et al., by guiding light at different frequencies using narrow structured domain walls inside an NLC, analogous to spin-dependent potentials for electrons in magnetized materials (Fig. 7(b)). As a result, they directly mapped the physics of spintronics into nonlinear optics [154].

While conventional phase-matching requirements often limit a crystal to a specific nonlinear process, atomically thin materials can relax these stringent conditions, opening new degrees of freedom [155]. For example, by tuning the pump wavelength and spectrally filtering the output, authors have demonstrated frequency conversion with both $\chi^{(2)}$ and $\chi^{(3)}$ nonlinearities in the same 2D crystal, enabling multiwavelength processes such as DFG, SFG, and four-wave mixing (FWM) [156], as depicted in Fig. 7(c).

Although second-order nonlinear ($\chi^{(2)}$) crystals such as $LiNbO_3$, KTP, and BBO remain the workhorses of nonlinear optics, but most usable $\chi^{(2)}$ crystals are synthetically fabricated [157]. In contrast, $\chi^{(3)}$ materials like silicon are naturally abundant and can be used directly to shape light [158]. As an example, recently, a silica-based glass slab (SiO_2) has been demonstrated for shaping light using FWM [159], where the new frequency beam was easily moved in and out of the focal plane by simply tailoring the pump's momentum vectors, in Fig. 7(d).

Beyond classical nonlinear mixing, metasurfaces can also serve as compact sources of quantum light, (Fig. 7(e)). Their sub-wavelength thickness relaxes phase-matching constraints, enabling broadband frequency conversion with enhanced local fields [160]. For instance, it is possible to achieve efficient and tunable SPDC with an enhancement factor of 10^2–10^4 using resonant metasurfaces supporting high Q factors [161]. However, traditional frequency conversion platforms are static, strictly designed for a chosen set of wavelengths. A solution to this is wavelength-adaptable nonlinear platforms, recently demonstrated with bimodal-shaping with an adjustable liquid crystal spin-orbit device [162] and tunable phase-matching in polarization-maintaining optical fibers [163]. An analogous approach achieved dynamic poling by electric field-induced shaping of $\chi^{(2)}$ domains in a $\chi^{(3)}$ medium, achieving reconfigurable control of spectral, spatial, and spatio-spectral degrees of freedom in real time [37], with an example shown in Fig. 7(f).

Finally, material transparency plays a crucial role. While $LiNbO_3$, KTP, and BBO are transparent from visible to mid-IR spectrum, they strongly absorb in the UV bands, limiting their use for frequency conversion in this band. Yet UV applications — particularly in spectroscopy, imaging, and biology — are highly desirable [164–166]. Here, recently, metasurfaces have emerged as a potential platform for efficient UV frequency conversion achieved by exploiting strong confinement within low-loss meta-atoms [167], allowing access to bulk nonlinearities and enabling compact optical elements such as deep-UV lenses [168], an example shown in Fig. 7(g).

6. FUTURE OUTLOOK

Revisiting nonlinear optics in the context of structured light has shifted the perspective both theoretically and experimentally. Theoretically, the introduction of structured waves rather than plane waves has given rise to new selection rules and paradigms. Light can diffract off light to create new radial modes, and OAM can be added or subtracted depending on the process. The introduction of mixed DoFs such as vectorial light has shown how both linear and nonlinear processes mix for new effects. What has made this possible is to challenge the paradigm of plane waves or Gaussian beams in the theoretical analysis, and we anticipate that as more assumptions are challenged, so will old processes be given a fresh perspective.

Experimentally, the shift has been away from wavelength conversion and the constraint of efficiency, instead of towards a new toolkit for the creation, control, and detection of multi-degree-of-freedom structured light. Extreme classical light has been used to open new regimes with structured light, from HHG to light with a self-torque. Power and intensity levels of structured light have also benefited from this revolution, now pushing Tera-watt levels. The new paradigms have enabled novel detection of structured light, ultra-fast correction of unwanted structure in structured light, and new creation tools. The introduction of structured nonlinearity together with structured light is a very exciting domain to watch, likely to compactify devices and improve functionality, e.g., tailoring the crystal for the light it will receive and the operation envisaged.

Yet there remain many open challenges. Most studies have remained at low power levels, not yet exploring control in new intensity regimes. This might be addressed by new bulk crystals and nonlinear resonant metasurfaces that can manage the power levels. At the opposite scale, quantum control is still limited by efficiency issues, prohibiting many quantum applications and protocols. This may be overcome with higher efficiencies from on-chip light confinement, and structured nonlinear matter to enhance particular state control. Applications have been impressive, but to make an impact, we need to speed up the deployment of nonlinear structured light from proof-of-principle demonstrations to real-world applications.

In this review, we have captured the recent progress in nonlinear structured light, illustrating with examples the exciting new trends and advances. In just a few years, we have witnessed advances in the field across many domains, pointing to a bright future where structured light and nonlinear structured materials combine to drive multi-dimensional light forward.

REFERENCES

[1] Forbes, A., M. de Oliveira, and M. R. Dennis, "Structured light," *Nature Photonics*, Vol. 15, No. 4, 253–262, 2021.

[2] Zhan, Q., "Spatiotemporal sculpturing of light: A tutorial," *Advances in Optics and Photonics*, Vol. 16, No. 2, 163–228, 2024.

[3] Yang, Y., A. Forbes, and L. Cao, "A review of liquid crystal spatial light modulators: Devices and applications," *Opto-Electronic Science*, Vol. 2, No. 8, 230026, 2023.

[4] Dorrah, A. H. and F. Capasso, "Tunable structured light with flat optics," *Science*, Vol. 376, No. 6591, eabi6860, 2022.

[5] Forbes, A. and I. Nape, "Quantum mechanics with patterns of light: Progress in high dimensional and multidimensional entanglement with structured light," *AVS Quantum Science*, Vol. 1, No. 1, 011701, 2019.
[6] Nape, I., B. Sephton, P. Ornelas, C. Moodley, and A. Forbes, "Quantum structured light in high dimensions," *APL Photonics*, Vol. 8, No. 5, 051101, 2023.
[7] Paúr, M., B. Stoklasa, Z. Hradil, L. L. Sánchez-Soto, and J. Rehacek, "Achieving the ultimate optical resolution," *Optica*, Vol. 3, No. 10, 1144–1147, 2016.
[8] Dorn, R., S. Quabis, and G. Leuchs, "Sharper focus for a radially polarized light beam," *Physical Review Letters*, Vol. 91, No. 23, 233901, Dec. 2003.
[9] Willner, A. E., K. Pang, H. Song, K. Zou, and H. Zhou, "Orbital angular momentum of light for communications," *Applied Physics Reviews*, Vol. 8, No. 4, 041312, 2021.
[10] Angelsky, O. V., A. Y. Bekshaev, S. G. Hanson, C. Y. Zenkova, I. I. Mokhun, and J. Zheng, "Structured light: Ideas and concepts," *Frontiers in Physics*, Vol. 8, 114, 2020.
[11] Wang, J. and Y. Liang, "Generation and detection of structured light: A review," *Frontiers in Physics*, Vol. 9, 688284, 2021.
[12] Cheng, M., W. Jiang, L. Guo, J. Li, and A. Forbes, "Metrology with a twist: Probing and sensing with vortex light," *Light: Science & Applications*, Vol. 14, No. 1, 4, 2025.
[13] Forbes, A., "Structured light from lasers," *Laser & Photonics Reviews*, Vol. 13, No. 11, 1900140, 2019.
[14] Forbes, A., L. Mkhumbuza, and L. Feng, "Orbital angular momentum lasers," *Nature Reviews Physics*, Vol. 6, No. 6, 352–364, 2024.
[15] Buono, W. T. and A. Forbes, "Nonlinear optics with structured light," *Opto-Electronic Advances*, Vol. 5, No. 6, 210174, 2022.
[16] Fang, Y., Z. Lyu, and Y. Liu, "Ultrafast physics with structured light," *Nature Reviews Physics*, Vol. 7, 713–727, 2025.
[17] Martín-Hernández, R., G. Gui, L. Plaja, H. C. Kapteyn, M. M. Murnane, C.-T. Liao, M. A. Porras, and C. Hernández-García, "Extreme-ultraviolet spatiotemporal vortices via high harmonic generation," *Nature Photonics*, Vol. 19, 817–824, 2025.
[18] Harrison, J., D. Naidoo, A. Forbes, and A. Dudley, "Progress in high-power and high-intensity structured light," *Advances in Physics: X*, Vol. 9, No. 1, 2327453, 2024.
[19] Carbajo, S., S.-W. Bahk, J. Baker, A. Bertozzi, A. Borthakur, A. Di Piazza, A. Forbes, S. Gessner, J. Hirschman, *et al.*, "Structured light at the extreme: Harnessing spatiotemporal control for high-field laser-matter interactions," *arXiv preprint arXiv:2512.05042*, 2025.
[20] Forbes, A., F. Nothlawala, and A. Vallés, "Progress in quantum structured light," *Nature Photonics*, Vol. 19, 1291–1300, 2025.
[21] Boyd, R. W., *Nonlinear Optics*, 3rd ed., 253–275, Academic Press, Burlington, 2008.
[22] Kovacic, I. and M. J. Brennan, *The Duffing Equation: Nonlinear Oscillators and Their Behaviour*, John Wiley & Sons, 2011.
[23] New, G., *Introduction to Nonlinear Optics*, Cambridge University Press, 2011.
[24] Barh, A., P. J. Rodrigo, L. Meng, C. Pedersen, and P. Tidemand-Lichtenberg, "Parametric upconversion imaging and its applications," *Advances in Optics and Photonics*, Vol. 11, No. 4, 952–1019, 2019.
[25] Emanueli, S. and A. Arie, "Temperature-dependent dispersion equations for $KTiOPO_4$ and $KTiOAsO_4$," *Applied Optics*, Vol. 42, No. 33, 6661–6665, 2003.
[26] Ma, J., X. Cheng, N. Zheng, P. Chen, X. Xu, T. Wang, D. Wei, Y. Nie, S. Zhu, M. Xiao, and Y. Zhang, "Fabrication of 100-nm-period domain structure in lithium niobate on insulator," *Optics Express*, Vol. 31, No. 23, 37 464–37 471, 2023.
[27] Singh, S., I. Nape, and A. Forbes, "Enhanced fidelity in nonlinear structured light by virtual light-based apertures," *Optics Express*, Vol. 33, No. 13, 27 615–27 625, 2025.
[28] De Oliveira, A. G., G. Santos, N. R. da Silva, L. J. Pereira, G. B. Alves, A. Z. Khoury, and P. H. S. Ribeiro, "Beyond conservation of orbital angular momentum in stimulated parametric down-conversion," *Physical Review Applied*, Vol. 16, No. 4, 044019, 2021.
[29] Yao, A. M. and M. J. Padgett, "Orbital angular momentum: Origins, behavior and applications," *Advances in Optics and Photonics*, Vol. 3, No. 2, 161–204, 2011.
[30] Chaitanya, N. A., M. V. Jabir, J. Banerji, and G. K. Samanta, "Hollow Gaussian beam generation through nonlinear interaction of photons with orbital angular momentum," *Scientific Reports*, Vol. 6, No. 1, 32464, 2016.
[31] Weiss, T. F. and A. Peruzzo, "Nonlinear domain engineering for quantum technologies," *Applied Physics Reviews*, Vol. 12, No. 1, 011318, 2025.
[32] Pertsch, T. and Y. Kivshar, "Nonlinear optics with resonant metasurfaces," *MRS Bulletin*, Vol. 45, No. 3, 210–220, 2020.
[33] Litchinitser, N. M., "Structured light meets structured matter," *Science*, Vol. 337, No. 6098, 1054–1055, 2012.
[34] Trajtenebrg-Mills, S. and A. Arie, "Shaping light beams in nonlinear processes using structured light and patterned crystals," *Optical Materials Express*, Vol. 7, No. 8, 2928–2942, 2017.
[35] Liu, H. and X. Chen, "The manipulation of second-order nonlinear harmonic wave by structured material and structured light," *Journal of Nonlinear Optical Physics & Materials*, Vol. 27, No. 4, 1850047, 2018.
[36] Disa, A. S., T. F. Nova, and A. Cavalleri, "Engineering crystal structures with light," *Nature Physics*, Vol. 17, No. 10, 1087–1092, 2021.
[37] Yanagimoto, R., B. A. Ash, M. M. Sohoni, M. M. Stein, Y. Zhao, F. Presutti, M. Jankowski, L. G. Wright, T. Onodera, and P. L. McMahon, "Programmable on-chip nonlinear photonics," *Nature*, 1–8, 2025.
[38] Qiu, X., F. Li, W. Zhang, Z. Zhu, and L. Chen, "Spiral phase contrast imaging in nonlinear optics: Seeing phase objects using invisible illumination," *Optica*, Vol. 5, No. 2, 208–212, 2018.
[39] Hong, L., F. Lin, X. Qiu, and L. Chen, "Second harmonic generation based joint transform correlator for human face and QR code recognitions," *Applied Physics Letters*, Vol. 116, No. 23, 231101, 2020.
[40] De Oliveira, A. G., M. F. Z. Arruda, W. C. Soares, S. P. Walborn, R. M. Gomes, R. M. de Araújo, and P. H. S. Ribeiro, "Real-time phase conjugation of vector vortex beams," *ACS Photonics*, Vol. 7, No. 1, 249–255, 2020.
[41] Zhu, Z., D. Zhang, F. Xie, J. Ma, J. Chen, S. Gong, W. Wu, W. Cai, X. Zhang, M. Ren, and J. Xu, "Nonlinear polarization imaging by parametric upconversion," *Optica*, Vol. 9, No. 11, 1297–1302, 2022.
[42] Jhajj, N., I. Larkin, E. W. Rosenthal, S. Zahedpour, J. K. Wahlstrand, and H. M. Milchberg, "Spatiotemporal optical vortices," *Physical Review X*, Vol. 6, No. 3, 031037, 2016.
[43] Yusufu, T., S. Niu, P. Tuersun, Y. Tulake, K. Miyamoto, and T. Omatsu, "Tunable 3 μm optical vortex parametric oscillator," *Japanese Journal of Applied Physics*, Vol. 57, No. 12, 122701, 2018.
[44] Gibbs, H., *Optical Bistability: Controlling Light With Light*, Elsevier, 2012.

[45] Desyatnikov, A. S. and A. I. Maimistov, "Interaction of two spatially separated light beams in a nonlinear Kerr medium," *Journal of Experimental and Theoretical Physics*, Vol. 86, No. 6, 1101–1106, 1998.

[46] Pura, B., J. Petykiewicz, L. Adamowicz, W. Jeda, M. Wierzbicki, and K. Brudzewski, "Polarisation control of light by light in a nonlinear polymer," *Applied Physics B*, Vol. 67, No. 2, 211–215, 1998.

[47] Zhang, J., K. F. MacDonald, and N. I. Zheludev, "Controlling light-with-light without nonlinearity," *Light: Science & Applications*, Vol. 1, No. 7, e18, 2012.

[48] Dholakia, K., N. B. Simpson, M. J. Padgett, and L. Allen, "Second-harmonic generation and the orbital angular momentum of light," *Physical Review A*, Vol. 54, No. 5, R3742, 1996.

[49] Wu, H.-J., H.-R. Yang, C. Rosales-Guzmán, W. Gao, B.-S. Shi, and Z.-H. Zhu, "Vectorial nonlinear optics: Type-II second-harmonic generation driven by spin-orbit-coupled fields," *Physical Review A*, Vol. 100, No. 5, 053840, 2019.

[50] Wang, J., F. Castellucci, and S. Franke-Arnold, "Vectorial light-matter interaction: Exploring spatially structured complex light fields," *AVS Quantum Science*, Vol. 2, No. 3, 031702, 2020.

[51] Wright, L. G., W. H. Renninger, D. N. Christodoulides, and F. W. Wise, "Nonlinear multimode photonics: Nonlinear optics with many degrees of freedom," *Optica*, Vol. 9, No. 7, 824–841, 2022.

[52] Buono, W. T., A. Santos, M. R. Maia, L. J. Pereira, D. S. Tasca, K. Dechoum, T. Ruchon, and A. Z. Khoury, "Chiral relations and radial-angular coupling in nonlinear interactions of optical vortices," *Physical Review A*, Vol. 101, No. 4, 043821, 2020.

[53] Wu, H.-J., L.-W. Mao, Y.-J. Yang, C. Rosales-Guzmán, W. Gao, B.-S. Shi, and Z.-H. Zhu, "Radial modal transitions of Laguerre-Gauss modes during parametric up-conversion: Towards the full-field selection rule of spatial modes," *Physical Review A*, Vol. 101, No. 6, 063805, 2020.

[54] Yang, H.-R., H.-J. Wu, W. Gao, C. Rosales-Guzmán, and Z.-H. Zhu, "Parametric upconversion of Ince-Gaussian modes," *Optics Letters*, Vol. 45, No. 11, 3034–3037, 2020.

[55] Steinlechner, F., N. Hermosa, V. Pruneri, and J. P. Torres, "Frequency conversion of structured light," *Scientific Reports*, Vol. 6, No. 1, 21390, 2016.

[56] Zdagkas, A., C. McDonnell, J. Deng, Y. Shen, G. Li, T. Ellenbogen, N. Papasimakis, and N. I. Zheludev, "Observation of toroidal pulses of light," *Nature Photonics*, Vol. 16, No. 7, 523–528, 2022.

[57] Abrahao, R. A., H. P. N. Morin, J. T. R. Pagé, A. Safari, R. W. Boyd, and J. S. Lundeen, "Shadow of a laser beam," *Optica*, Vol. 11, No. 11, 1549–1555, 2024.

[58] Fickler, R., L. Kopf, and M. Ornigotti, "Higher-order Poincaré spheres and spatiospectral Poincaré beams," *Physical Review Research*, Vol. 6, No. 3, 033298, 2024.

[59] Gariepy, G., "Conservation of orbital angular momentum in high-harmonic generation," MSc thesis, University of Ottawa, Ottawa, Canada, 2013.

[60] Rego, L., K. M. Dorney, N. J. Brooks, Q. L. Nguyen, C.-T. Liao, J. S. Román, D. E. Couch, A. Liu, E. Pisanty, M. Lewenstein, *et al.*, "Generation of extreme-ultraviolet beams with time-varying orbital angular momentum," *Science*, Vol. 364, No. 6447, eaaw9486, 2019.

[61] Li, X. F., A. L'Huillier, M. Ferray, L. A. Lompré, and G. Mainfray, "Multiple-harmonic generation in rare gases at high laser intensity," *Physical Review A*, Vol. 39, No. 11, 5751, 1989.

[62] Gao, J., X. Zhang, Y. Wang, Y. Fang, Q. Lu, Z. Li, Y. Liu, C. Wu, Q. Gong, Y. Liu, and H. Jiang, "Structured air lasing of N_2^+," *Communications Physics*, Vol. 6, No. 1, 97, 2023.

[63] Srinivasa Rao, A., K. Miamoto, and T. Omatsu, "Ultraviolet intracavity frequency-doubled Pr^{3+} : $LiYF_4$ orbital Poincaré laser," *Optics Express*, Vol. 28, No. 25, 37 397–37 405, 2020.

[64] Alam, S. U., A. S. Rao, A. Ghosh, P. Vaity, and G. K. Samanta, "Nonlinear frequency doubling characteristics of asymmetric vortices of tunable, broad orbital angular momentum spectrum," *Applied Physics Letters*, Vol. 112, No. 17, 171102, 2018.

[65] Pan, J.-T., B.-H. Zhu, L.-L. Ma, W. Chen, G.-Y. Zhang, J. Tang, Y. Liu, Y. Wei, C. Zhang, Z.-H. Zhu, *et al.*, "Nonlinear geometric phase coded ferroelectric nematic fluids for nonlinear soft-matter photonics," *Nature Communications*, Vol. 15, No. 1, 8732, 2024.

[66] De Ceglia, D., L. Coudrat, I. Roland, M. A. Vincenti, M. Scalora, R. Tanos, J. Claudon, J.-M. Gérard, A. Degiron, G. Leo, and C. de Angelis, "Nonlinear spin-orbit coupling in optical thin films," *Nature Communications*, Vol. 15, No. 1, 1625, 2024.

[67] Ren, Z.-C., Y.-C. Lou, Z.-M. Cheng, L. Fan, J. Ding, X.-L. Wang, and H.-T. Wang, "Optical frequency conversion of light with maintaining polarization and orbital angular momentum," *Optics Letters*, Vol. 46, No. 10, 2300–2303, 2021.

[68] Pinheiro da Silva, B., W. T. Buono, L. J. Pereira, D. S. Tasca, K. Dechoum, and A. Z. Khoury, "Spin to orbital angular momentum transfer in frequency up-conversion," *Nanophotonics*, Vol. 11, No. 4, 771–778, 2022.

[69] Samim, M., S. Krouglov, and V. Barzda, "Nonlinear stokes-mueller polarimetry," *Physical Review A*, Vol. 93, No. 1, 013847, 2016.

[70] Chen, H., G. Liu, S. Zhang, Y. Zhong, J. Yu, Z. Chen, and W. Zhu, "Spin Hall effect of nonlinear photons," *Laser & Photonics Reviews*, Vol. 17, No. 5, 2200681, 2023.

[71] Tang, Y., Z. Hu, J. Deng, K. Li, and G. Li, "Sequential harmonic spin-orbit angular momentum generation in nonlinear optical crystals," *Opto-Electronic Advances*, Vol. 7, No. 12, 240138, 2025.

[72] Tang, Y., K. Li, X. Zhang, J. Deng, G. Li, and E. Brasselet, "Harmonic spin-orbit angular momentum cascade in nonlinear optical crystals," *Nature Photonics*, Vol. 14, No. 11, 658–662, 2020.

[73] Li, Y., Z.-Y. Zhou, D.-S. Ding, and B.-S. Shi, "Sum frequency generation with two orbital angular momentum carrying laser beams," *Journal of the Optical Society of America B*, Vol. 32, No. 3, 407–411, 2015.

[74] Aguilar-Cardoso, A. A., C. Li, T. J. B. Luck, M. F. Ferrer-Garcia, J. Upham, J. S. Lundeen, and R. W. Boyd, "Tailoring spatial modes produced by stimulated parametric down-conversion," *Physical Review A*, Vol. 112, No. 4, 043541, 2025.

[75] Wu, H.-J., B.-S. Yu, J.-Q. Jiang, C.-Y. Li, C. Rosales-Guzmán, S.-L. Liu, Z.-H. Zhu, and B.-S. Shi, "Observation of anomalous orbital angular momentum transfer in parametric nonlinearity," *Physical Review Letters*, Vol. 130, No. 15, 153803, 2023.

[76] Kumar, S., R. K. Saripalli, A. Ghosh, W. T. Buono, A. Forbes, and G. K. Samanta, "Controlling the coverage of full Poincaré beams through second-harmonic generation," *Physical Review Applied*, Vol. 19, No. 3, 034082, 2023.

[77] Liu, H., H. Li, Y. Zheng, and X. Chen, "Nonlinear frequency conversion and manipulation of vector beams," *Optics Letters*, Vol. 43, No. 24, 5981–5984, 2018.

[78] Luttmann, M., M. Vimal, M. Guer, J.-F. Hergott, A. Z. Khoury, C. Hernández-García, E. Pisanty, and T. Ruchon, "Nonlinear up-conversion of a polarization mobius strip with half-integer optical angular momentum," *Science Advances*, Vol. 9, No. 12,

eadf3486, 2023.

[79] Da Motta, M. R. L., G. B. Alves, A. Z. Khoury, and S. S. Vianna, "Poincaré-sphere symmetries in four-wave mixing with orbital angular momentum," *Physical Review A*, Vol. 109, No. 1, 013506, 2024.

[80] Pan, C., H. Li, H. Pang, R. Ru, S. Zhang, D. Wei, H. Chen, H. Gao, and F. Li, "Generation and manipulation of spin-orbit coupling mode via four-wave mixing with quantum interference," *Laser & Photonics Reviews*, Vol. 18, No. 2, 2300625, 2024.

[81] Pan, C., H. Li, X. Zhang, Y. Liu, L. Wu, H. Pang, H. Chen, D. Wei, H. Gao, and F. Li, "All-optical controlled multichannel nonlinear holography for switchable beam shaping in an atomic vapor," *Optica*, Vol. 12, No. 7, 1054–1060, 2025.

[82] Yuan, J., X. Wang, G. Chen, L. Wang, L. Xiao, and S. Jia, "High-fidelity frequency converter in high-dimensional spaces," *Laser & Photonics Reviews*, Vol. 18, No. 11, 2400368, 2024.

[83] Gao, W., S. Wang, J. Yuan, L. Wang, L. Xiao, and S. Jia, "High-contrast nonlinear spiral phase contrast imaging via four-wave mixing in atomic medium," *Optics Express*, Vol. 33, No. 18, 38 382–38 391, 2025.

[84] Bornman, N., W. T. Buono, M. Lovemore, and A. Forbes, "Optimal pump shaping for entanglement control in any countable basis," *Advanced Quantum Technologies*, Vol. 4, No. 10, 2100066, 2021.

[85] Jabir, M. V., N. A. Chaitanya, A. Aadhi, and G. K. Samanta, "Generation of "perfect" vortex of variable size and its effect in angular spectrum of the down-converted photons," *Scientific Reports*, Vol. 6, No. 1, 21877, 2016.

[86] Nirala, G., S. T. Pradyumna, A. Kumar, and A. M. Marino, "Information encoding in the spatial correlations of entangled twin beams," *Science Advances*, Vol. 9, No. 22, eadf9161, 2023.

[87] Rozenberg, E., A. Karnieli, O. Yesharim, J. Foley-Comer, S. Trajtenberg-Mills, D. Freedman, A. M. Bronstein, and A. Arie, "Inverse design of spontaneous parametric downconversion for generation of high-dimensional qudits," *Optica*, Vol. 9, No. 6, 602–615, 2022.

[88] Kysela, J., M. Erhard, A. Hochrainer, M. Krenn, and A. Zeilinger, "Path identity as a source of high-dimensional entanglement," *Proceedings of the National Academy of Sciences*, Vol. 117, No. 42, 26 118–26 122, 2020.

[89] Trovatello, C., A. Marini, M. Cotrufo, A. Alù, P. J. Schuck, and G. Cerullo, "Tunable optical nonlinearities in layered materials," *ACS Photonics*, Vol. 11, No. 8, 2860–2873, 2024.

[90] Yesharim, O., I. Hurvitz, J. Foley-Comer, and A. Arie, "Bulk nonlinear metamaterials for generation of quantum light," *Applied Physics Reviews*, Vol. 12, No. 1, 011323, 2025.

[91] Huang, J. H. and P. Kumar, "Observation of quantum frequency conversion," *Physical Review Letters*, Vol. 68, 2153, 1992.

[92] Vandevender, A. P. and P. G. Kwiat, "High efficiency single photon detection via frequency up-conversion," *Journal of Modern Optics*, Vol. 51, No. 9-10, 1433–1445, 2004.

[93] Zaske, S., A. Lenhard, C. A. Keßler, J. Kettler, C. Hepp, C. Arend, R. Albrecht, W.-M. Schulz, M. Jetter, P. Michler, and C. Becher, "Visible-to-telecom quantum frequency conversion of light from a single quantum emitter," *Physical Review Letters*, Vol. 109, No. 14, 147404, 2012.

[94] Ansari, V., J. M. Donohue, B. Brecht, and C. Silberhorn, "Tailoring nonlinear processes for quantum optics with pulsed temporal-mode encodings," *Optica*, Vol. 5, No. 5, 534–550, 2018.

[95] Eckstein, A., B. Brecht, and C. Silberhorn, "A quantum pulse gate based on spectrally engineered sum frequency generation," *Optics Express*, Vol. 19, No. 15, 13 770–13 778, 2011.

[96] Ansari, V., J. M. Donohue, M. Allgaier, L. Sansoni, B. Brecht, J. Roslund, N. Treps, G. Harder, and C. Silberhorn, "Tomography and purification of the temporal-mode structure of quantum light," *Physical Review Letters*, Vol. 120, No. 21, 213601, 2018.

[97] Serino, L., J. Gil-Lopez, M. Stefszky, R. Ricken, C. Eigner, B. Brecht, and C. Silberhorn, "Realization of a multi-output quantum pulse gate for decoding high-dimensional temporal modes of single-photon states," *PRX Quantum*, Vol. 4, No. 2, 020306, 2023.

[98] Serino, L., C. Eigner, B. Brecht, and C. Silberhorn, "Programmable time-frequency mode-sorting of single photons with a multi-output quantum pulse gate," *Optics Express*, Vol. 33, No. 3, 5577–5586, 2025.

[99] Donohue, J. M., M. Agnew, J. Lavoie, and K. J. Resch, "Coherent ultrafast measurement of time-bin encoded photons," *Physical Review Letters*, Vol. 111, 153602, 2013.

[100] Allgaier, M., V. Ansari, J. M. Donohue, C. Eigner, V. Quiring, R. Ricken, B. Brecht, and C. Silberhorn, "Pulse shaping using dispersion-engineered difference frequency generation," *Physical Review A*, Vol. 101, No. 4, 043819, 2020.

[101] Sephton, B., A. Vallés, I. Nape, M. A. Cox, F. Steinlechner, T. Konrad, J. P. Torres, F. S. Roux, and A. Forbes, "Quantum transport of high-dimensional spatial information with a nonlinear detector," *Nature Communications*, Vol. 14, No. 1, 8243, 2023.

[102] Qiu, X., H. Guo, and L. Chen, "Remote transport of high-dimensional orbital angular momentum states and ghost images via spatial-mode-engineered frequency conversion," *Nature Communications*, Vol. 14, No. 1, 8244, 2023.

[103] Tsujimoto, Y., K. Wakui, T. Kishimoto, S. Miki, M. Yabuno, H. Terai, M. Fujiwara, and G. Kato, "Experimental entanglement swapping through single-photon $\chi^{(2)}$ nonlinearity," *Nature Communications*, Vol. 16, No. 1, 8720, 2025.

[104] Akin, J., Y. Zhao, P. G. Kwiat, E. A. Goldschmidt, and K. Fang, "Faithful quantum teleportation via a nanophotonic nonlinear Bell state analyzer," *Physical Review Letters*, Vol. 134, No. 16, 160802, 2025.

[105] Ackermann, L., C. Roider, K. Cvecek, N. Barré, C. Aigner, and M. Schmidt, "Polarization-controlled nonlinear computer-generated holography," *Scientific Reports*, Vol. 13, No. 1, 10338, 2023.

[106] Tamura, R., P. Kumar, A. S. Rao, K. Tsuda, F. Getzlaff, K. Miyamoto, N. M. Litchinitser, and T. Omatsu, "Direct imprint of optical skyrmions in azopolymers as photoinduced relief structures," *APL Photonics*, Vol. 9, No. 4, 046104, 2024.

[107] Trajtenberg-Mills, S., I. Juwiler, and A. Arie, "On-axis shaping of second-harmonic beams," *Laser & Photonics Reviews*, Vol. 9, No. 6, L40–L44, 2015.

[108] Wang, M., Y. Li, Y. Tang, J. Chen, R. Rong, G. Li, T. Cao, and S. Chen, "Nonlinear chiroptical holography with Pancharatnam-Berry phase controlled plasmonic metasurface," *Laser & Photonics Reviews*, Vol. 16, No. 12, 2200350, 2022.

[109] Coudrat, L., G. Boulliard, J.-M. Gérard, A. Lemaître, A. Degiron, and G. Leo, "Unravelling the nonlinear generation of designer vortices with dielectric metasurfaces," *Light: Science & Applications*, Vol. 14, No. 1, 51, 2025.

[110] Rong, R., Y. Li, M. Wang, Y. Tang, H. Xu, K. Li, G. Li, T. Cao, and S. Chen, "Beam steering of nonlinear optical vortices with phase gradient plasmonic metasurfaces," *ACS Photonics*, Vol. 10, No. 9, 3248–3254, 2023.

[111] Park, S., J. Yu, G. Boehm, M. A. Belkin, and J. Lee, "Electrically tunable third-harmonic generation using intersubband polaritonic metasurfaces," *Light: Science & Applications*, Vol. 13, No. 1, 169, 2024.

[112] Zhang, X., H. Li, S. Liu, Y. Chen, Z. Zhu, H. Liu, S. Zhu, and X. Hu, "Tailoring beam profile and OAM spectrum in domain-engineered nonlinear photonic crystals," *APL Photonics*, Vol. 10, No. 1, 010802, 2025.

[113] Yang, J.-C., W. Chen, L.-L. Ma, A.-Z. Yu, J.-T. Pan, J.-T. Fan, M.-L. Hu, and Y.-Q. Lu, "Nonlinear photon sieves for high-fidelity wavefront engineering," *Laser & Photonics Reviews*, Vol. 19, No. 22, e01117, 2025.

[114] Yesharim, O., S. Pearl, J. Foley-Comer, I. Juwiler, and A. Arie, "Direct generation of spatially entangled qudits using quantum nonlinear optical holography," *Science Advances*, Vol. 9, No. 8, eade7968, 2023.

[115] Ye, Z., W. Hou, C.-X. Ding, X.-J. Men, R.-J. He, J. Zhao, H.-B. Wang, J. Xiong, and K. Wang, "Random holography: Generating EPR-like correlation with thermal photons," *Laser & Photonics Reviews*, Vol. 19, No. 6, 2401610, 2025.

[116] Hou, W., R.-J. He, Z. Ye, X.-J. Men, C.-X. Ding, H.-C. Liu, H.-B. Wang, and J. Xiong, "Manipulating classical triple correlations for optical information processing and metrology," *Photonics Research*, Vol. 13, No. 8, 2073–2087, 2025.

[117] Lukens, J. M., A. Dezfooliyan, C. Langrock, M. M. Fejer, D. E. Leaird, and A. M. Weiner, "Orthogonal spectral coding of entangled photons," *Physical Review Letters*, Vol. 112, No. 13, 133602, 2014.

[118] Xu, Y., S. Tang, A. N. Black, and R. W. Boyd, "Orthogonal spatial coding with stimulated parametric down-conversion," *Optics Express*, Vol. 31, No. 25, 42 723–42 729, 2023.

[119] Qi, T., Y.-Z. Chen, D. Yan, and W. Gao, "Wavefront-reversal, low-threshold, and enhanced stimulated brillouin scattering for arbitrary structured light," *Laser & Photonics Reviews*, Vol. 18, No. 6, 2301080, 2024.

[120] Singh, S., B. Sephton, W. T. Buono, V. D'Ambrosio, T. Konrad, and A. Forbes, "Light correcting light with nonlinear optics," *Advanced Photonics*, Vol. 6, No. 2, 026003, 2024.

[121] Zhou, H., X. Su, Y. Duan, Y. Zuo, Z. Jiang, M. Ramakrishnan, J. Tepper, V. Ziegler, R. W. Boyd, M. Tur, and A. E. Willner, "Automatic mitigation of dynamic atmospheric turbulence using optical phase conjugation for coherent free-space optical communications," *Optica*, Vol. 12, No. 2, 158–167, 2025.

[122] Sánchez-Montes, A. R., S. Singh, A. Márquez, J. Francés, A. Forbes, and A. Dudley, "Nonlinear modal decomposition of structured light," *Optics Express*, Vol. 33, No. 19, 41 261–41 270, 2025.

[123] Moon, J., Y.-C. Cho, S. Kang, M. Jang, and W. Choi, "Measuring the scattering tensor of a disordered nonlinear medium," *Nature Physics*, Vol. 19, No. 11, 1709–1718, 2023.

[124] Sohmen, M., M. Borozdova, M. Ritsch-Marte, and A. Jesacher, "Complex-valued scatter compensation in nonlinear microscopy," *Physical Review Applied*, Vol. 22, No. 4, 044036, 2024.

[125] Buono, W. T., J. Santiago, L. J. Pereira, D. S. Tasca, K. Dechoum, and A. Z. Khoury, "Polarization-controlled orbital angular momentum switching in nonlinear wave mixing," *Optics Letters*, Vol. 43, No. 7, 1439–1442, 2018.

[126] Pereira, L. J., W. T. Buono, D. S. Tasca, K. Dechoum, and A. Z. Khoury, "Orbital-angular-momentum mixing in type-II second-harmonic generation," *Physical Review A*, Vol. 96, No. 5, 053856, 2017.

[127] Wu, H.-J., B. Zhao, C. Rosales-Guzmán, W. Gao, B.-S. Shi, and Z.-H. Zhu, "Spatial-polarization-independent parametric up-conversion of vectorially structured light," *Physical Review Applied*, Vol. 13, No. 6, 064041, 2020.

[128] Pinheiro da Silva, B., G. H. dos Santos, A. G. de Oliveira, N. R. da Silva, W. T. Buono, R. M. Gomes, W. C. Soares, A. J. Jesus-Silva, E. J. S. Fonseca, P. H. S. Ribeiro, and A. Z. Khoury, "Observation of a triangular-lattice pattern in nonlinear wave mixing with optical vortices," *Optica*, Vol. 9, No. 8, 908–912, 2022.

[129] Wu, H.-J., B.-S. Yu, Z.-H. Zhu, W. Gao, D.-S. Ding, Z.-Y. Zhou, X.-P. Hu, C. Rosales-Guzmán, Y. Shen, and B.-S. Shi, "Conformal frequency conversion for arbitrary vectorial structured light," *Optica*, Vol. 9, No. 2, 187–196, 2022.

[130] Menshikov, E., P. Franceschini, K. Frizyuk, I. Fernandez-Corbaton, A. Tognazzi, A. C. Cino, D. Garoli, M. Petrov, D. de Ceglia, and C. de Angelis, "Light structuring via nonlinear total angular momentum addition with flat optics," *Light: Science & Applications*, Vol. 14, No. 1, 381, 2025.

[131] Zhang, Y., Y. Sheng, S. Zhu, M. Xiao, and W. Krolikowski, "Nonlinear photonic crystals: From 2D to 3D," *Optica*, Vol. 8, No. 3, 372–381, 2021.

[132] Chen, P., C. Wang, D. Wei, Y. Hu, X. Xu, J. Li, D. Wu, J. Ma, S. Ji, L. Zhang, *et al.*, "Quasi-phase-matching-division multiplexing holography in a three-dimensional nonlinear photonic crystal," *Light: Science & Applications*, Vol. 10, No. 1, 146, 2021.

[133] Olarte, O. E., J. Licea-Rodriguez, J. A. Palero, E. J. Gualda, D. Artigas, J. Mayer, J. Swoger, J. Sharpe, I. Rocha-Mendoza, R. Rangel-Rojo, and P. Loza-Alvarez, "Image formation by linear and nonlinear digital scanned light-sheet fluorescence microscopy with Gaussian and Bessel beam profiles," *Biomedical Optics Express*, Vol. 3, No. 7, 1492–1505, 2012.

[134] Vettenburg, T., H. I. C. Dalgarno, J. Nylk, C. Coll-Lladó, D. E. K. Ferrier, T. Čižmár, F. J. Gunn-Moore, and K. Dholakia, "Light-sheet microscopy using an Airy beam," *Nature Methods*, Vol. 11, No. 5, 541–544, 2014.

[135] Valle, A. F. and J. D. Seelig, "Two-photon Bessel beam tomography for fast volume imaging," *Optics Express*, Vol. 27, No. 9, 12 147–12 162, 2019.

[136] Chen, X., S. Zhong, Y. Hou, R. Cao, W. Wang, D. Li, Q. Dai, D. Kim, and P. Xi, "Superresolution structured illumination microscopy reconstruction algorithms: A review," *Light: Science & Applications*, Vol. 12, No. 1, 172, 2023.

[137] Zhang, C., B. Yu, F. Lin, S. Samanta, H. Yu, W. Zhang, Y. Jing, C. Shang, D. Lin, K. Si, W. Gong, and J. Qu, "Deep tissue super-resolution imaging with adaptive optical two-photon multifocal structured illumination microscopy," *PhotoniX*, Vol. 4, No. 1, 38, 2023.

[138] Lee, H., H. Yoo, G. Moon, K.-A. Toh, K. Mochizuki, K. Fujita, and D. Kim, "Super-resolved Raman microscopy using random structured light illumination: Concept and feasibility," *The Journal of Chemical Physics*, Vol. 155, No. 14, 144202, 2021.

[139] Wang, F., Y. Zhong, O. Bruns, Y. Liang, and H. Dai, "In vivo NIR-II fluorescence imaging for biology and medicine," *Nature Photonics*, Vol. 18, No. 6, 535–547, 2024.

[140] Badrodien, I., P. H. Neethling, and G. W. Bosman, "Improved image contrast in nonlinear light-sheet fluorescence microscopy using i^2PIE Pulse compression," *Scientific Reports*, Vol. 14, No. 1, 12770, 2024.

[141] Barsi, C., W. Wan, and J. W. Fleischer, "Imaging through nonlinear media using digital holography," *Nature Photonics*,

Vol. 3, No. 4, 211–215, 2009.

[142] Jia, S., J. Lee, J. W. Fleischer, G. A. Siviloglou, and D. N. Christodoulides, "Diffusion-trapped Airy beams in photorefractive media," *Physical Review Letters*, Vol. 104, No. 25, 253904, 2010.

[143] Cao, J., D. Shen, Y. Feng, and W. Wan, "Nonlinear negative refraction by difference frequency generation," *Applied Physics Letters*, Vol. 108, No. 19, 191101, 2016.

[144] Xu, X., P. Chen, T. Ma, J. Ma, C. Zhou, Y. Su, M. Lv, W. Fan, B. Zhai, Y. Sun, *et al.*, "Large field-of-view nonlinear holography in lithium niobate," *Nano Letters*, Vol. 24, No. 4, 1303–1308, 2024.

[145] Shen, F., W. Fan, Y. Zhang, X. Chen, and Y. Chen, "3D orbital angular momentum nonlinear holography," *Advanced Optical Materials*, Vol. 13, No. 9, 2402836, 2025.

[146] Chen, Y.-Z., D. Yan, T. Qi, X.-W. Wang, and W. Gao, "Observation of spatial differentiation in structured nonlinear optics," *Laser & Photonics Reviews*, Vol. 19, No. 20, e00595, 2025.

[147] Sun, X., H. Wu, B. Gao, C. Wang, Y. Ma, X. Hong, C. Zhang, Y. Qin, and Y. Zhu, "Observation of ferroelectric domain walls using nonlinear spiral interferometry," *Applied Physics Letters*, Vol. 125, No. 7, 071111, 2024.

[148] Wang, C., Z. Li, M.-H. Kim, X. Xiong, X.-F. Ren, G.-C. Guo, N. Yu, and M. Lončar, "Metasurface-assisted phase-matching-free second harmonic generation in lithium niobate waveguides," *Nature Communications*, Vol. 8, No. 1, 2098, 2017.

[149] Dutt, A., A. Mohanty, A. L. Gaeta, and M. Lipson, "Nonlinear and quantum photonics using integrated optical materials," *Nature Reviews Materials*, Vol. 9, No. 5, 321–346, 2024.

[150] Gao, J., M. A. Vincenti, J. Frantz, A. Clabeau, X. Qiao, L. Feng, M. Scalora, and N. M. Litchinitser, "Near-infrared to ultraviolet frequency conversion in chalcogenide metasurfaces," *Nature Communications*, Vol. 12, No. 1, 5833, 2021.

[151] Zheng, Z., D. Smirnova, G. Sanderson, Y. Cuifeng, D. C. Koutsogeorgis, L. Huang, Z. Liu, R. Oulton, A. Yousefi, A. E. Miroshnichenko, *et al.*, "Broadband infrared imaging governed by guided-mode resonance in dielectric metasurfaces," *Light: Science & Applications*, Vol. 13, No. 1, 249, 2024.

[152] Gao, J., H. B. Sedeh, D. Tsvetkov, D. G. Pires, M. A. Vincenti, Y. Xu, I. Kravchenko, R. George, M. Scalora, L. Feng, *et al.*, "Topology-imprinting in nonlinear metasurfaces," *Science Advances*, Vol. 11, No. 24, eadv5190, 2025.

[153] Vabishchevich, P. and Y. Kivshar, "Nonlinear photonics with metasurfaces," *Photonics Research*, Vol. 11, No. 2, B50–B64, 2023.

[154] Yesharim, O., S. Izhak, and A. Arie, "Pseudo-spin light circuits in nonlinear photonic crystals," *Nature Communications*, Vol. 16, No. 1, 6508, 2025.

[155] Autere, A., H. Jussila, Y. Dai, Y. Wang, H. Lipsanen, and Z. Sun, "Nonlinear optics with 2D layered materials," *Advanced Materials*, Vol. 30, No. 24, 1705963, 2018.

[156] Norden, T., L. M. Martinez, N. Tarefder, K. W. C. Kwock, L. M. McClintock, N. Olsen, L. N. Holtzman, J. H. Yeo, L. Zhao, X. Zhu, *et al.*, "Twisted nonlinear optics in monolayer van der Waals crystals," *ACS Nano*, Vol. 19, No. 34, 30 919–30 929, 2025.

[157] Dang, J., D. Mei, and Y. Wu, "Review of growth method for typical nonlinear optical crystal," *Journal of Synthetic Crystals*, Vol. 49, No. 7, 1308, 2020.

[158] Borghi, M., C. Castellan, S. Signorini, A. Trenti, and L. Pavesi, "Nonlinear silicon photonics," *Journal of Optics*, Vol. 19, No. 9, 093002, 2017.

[159] Shen, D., J. Cao, and W. Wan, "Wavefront shaping with nonlinear four-wave mixing," *Scientific Reports*, Vol. 13, No. 1, 2750, 2023.

[160] Keren-Zur, S., L. Michaeli, H. Suchowski, and T. Ellenbogen, "Shaping light with nonlinear metasurfaces," *Advances in Optics and Photonics*, Vol. 10, No. 1, 309–353, 2018.

[161] Santiago-Cruz, T., S. D. Gennaro, O. Mitrofanov, S. Addamane, J. Reno, I. Brener, and M. V. Chekhova, "Resonant metasurfaces for generating complex quantum states," *Science*, Vol. 377, No. 6609, 991–995, 2022.

[162] Dekkers, K., M. Koni, V. Hakobyan, S. Singh, J. Leach, E. Brasselet, I. Nape, and A. Forbes, "Wavelength-adaptive spin-orbit orbital angular momentum management in three-wave mixing," *Journal of Optics*, Vol. 27, No. 11, 115501, 2025.

[163] Bashan, G., A. Eyal, M. Tur, and A. Arie, "Optically programable quasi phase matching in four-wave mixing," *Nature Communications*, Vol. 16, No. 1, 6855, 2025.

[164] Vasilets, V. N., A. V. Kuznetsov, and V. I. Sevastianov, "Vacuum ultraviolet treatment of polyethylene to change surface properties and characteristics of protein adsorption," *Journal of Biomedical Materials Research Part A: An Official Journal of the Society for Biomaterials, The Japanese Society for Biomaterials, and the Australian Society for Biomaterials and the Korean Society for Biomaterials*, Vol. 69, No. 3, 428–435, 2004.

[165] Mao, Y., D. Zhao, S. Yan, H. Zhang, J. Li, K. Han, X. Xu, C. Guo, L. Yang, C. Zhang, K. Huang, and Y. Chen, "A vacuum ultraviolet laser with a submicrometer spot for spatially resolved photoemission spectroscopy," *Light: Science & Applications*, Vol. 10, No. 1, 22, 2021.

[166] Wang, J., Z. Wang, F. Liu, L. Cai, J.-B. Pan, Z. Li, S. Zhang, H.-Y. Chen, X. Zhang, and Y. Mo, "Vacuum ultraviolet laser desorption/ionization mass spectrometry imaging of single cells with submicron craters," *Analytical Chemistry*, Vol. 90, No. 16, 10 009–10 015, 2018.

[167] Semmlinger, M., M. L. Tseng, J. Yang, M. Zhang, C. Zhang, W.-Y. Tsai, D. P. Tsai, P. Nordlander, and N. J. Halas, "Vacuum ultraviolet light-generating metasurface," *Nano Letters*, Vol. 18, No. 9, 5738–5743, 2018.

[168] Tseng, M. L., M. Semmlinger, M. Zhang, C. Arndt, T.-T. Huang, J. Yang, H. Y. Kuo, V.-C. Su, M. K. Chen, C. H. Chu, *et al.*, "Vacuum ultraviolet nonlinear metalens," *Science Advances*, Vol. 8, No. 16, eabn5644, 2022.

[169] Reintjes, J. and R. C. Eckardt, "Efficient harmonic generation from 532 to 266 nm in ADP and KD*P," *Applied Physics Letters*, Vol. 30, No. 2, 91–93, 1977.

[170] Sakuma, J., Y. Asakawa, and M. Obara, "Generation of 5-W deep-UV continuous-wave radiation at 266 nm by an external cavity with a $CsLiB_6O_{10}$ crystal," *Optics Letters*, Vol. 29, No. 1, 92–94, 2004.

[171] Zhang, J.-W., H.-N. Han, L. Hou, L. Zhang, Z.-J. Yu, D.-H. Li, and Z.-Y. Wei, "Frequency doubled femtosecond Ti : sapphire laser with an assisted enhancement cavity," *Chinese Physics B*, Vol. 25, No. 1, 014205, 2016.

[172] Ghorui, C., A. M. Rudra, U. Chatterjee, A. K. Chaudhary, and D. Ganesh, "Efficient second-harmonic and terahertz generation from single BiB_3O_6 crystal using nanosecond and femtosecond lasers," *Applied Optics*, Vol. 60, No. 19, 5643–5651, 2021.

[173] Kang, L., H. Bao, and D. H. Werner, "Efficient second-harmonic generation in high Q-factor asymmetric lithium niobate metasurfaces," *Optics Letters*, Vol. 46, No. 3, 633–636, 2021.

[174] Liu, S., M. B. Sinclair, S. Saravi, G. A. Keeler, Y. Yang, J. Reno, G. M. Peake, F. Setzpfandt, I. Staude, T. Pertsch, and I. Brener, "Resonantly enhanced second-harmonic generation using III-V semiconductor all-dielectric metasurfaces," *Nano Letters*, Vol. 16, No. 9, 5426–5432, 2016.

[175] Vabishchevich, P. P., S. Liu, M. B. Sinclair, G. A. Keeler, G. M. Peake, and I. Brener, "Enhanced second-harmonic generation using broken symmetry III-V semiconductor Fano metasurfaces," *ACS Photonics*, Vol. 5, No. 5, 1685–1690, 2018.

[176] Li, J., G. Hu, L. Shi, N. He, D. Li, Q. Shang, Q. Zhang, H. Fu, L. Zhou, W. Xiong, *et al.*, "Full-color enhanced second harmonic generation using rainbow trapping in ultrathin hyperbolic metamaterials," *Nature Communications*, Vol. 12, No. 1, 6425, 2021.

[177] Brown, A. J. W., M. S. Bowers, K. W. Kangas, and C. H. Fisher, "High-energy, high-efficiency second-harmonic generation of 1064-nm radiation in KTP," *Optics Letters*, Vol. 17, No. 2, 109–111, 1992.

[178] Kumar, S. C., G. K. Samanta, K. Devi, and M. Ebrahim-Zadeh, "High-efficiency, multicrystal, single-pass, continuous-wave second harmonic generation," *Optics Express*, Vol. 19, No. 12, 11 152–11 169, 2011.

[179] Liu, H.-Y., Z.-H. Zhou, Q. Bian, Y. Bo, Y. Kou, L. Yuan, D.-F. Cui, and Q.-J. Peng, "High-efficiency nanosecond green laser based on extra-cavity second-harmonic generation of a Nd : YAG MOPA system," *IEEE Photonics Journal*, Vol. 15, No. 5, 1–5, 2023.

[180] Gwo, S., C.-Y. Wang, H.-Y. Chen, M.-H. Lin, L. Sun, X. Li, W.-L. Chen, Y.-M. Chang, and H. Ahn, "Plasmonic metasurfaces for nonlinear optics and quantitative SERS," *ACS Photonics*, Vol. 3, No. 8, 1371–1384, 2016.

[181] Suntsov, S., C. E. Rüter, D. Brüske, and D. Kip, "Watt-level 775 nm SHG with 70% conversion efficiency and 97% pump depletion in annealed/reverse proton exchanged diced PPLN ridge waveguides," *Optics Express*, Vol. 29, No. 8, 11 386–11 393, 2021.

[182] Gili, V. F., L. Carletti, A. Locatelli, D. Rocco, M. Finazzi, L. Ghirardini, I. Favero, C. Gomez, A. Lemaître, M. Celebrano, C. de Angelis, and G. Leo, "Monolithic AlGaAs second-harmonic nanoantennas," *Optics Express*, Vol. 24, No. 14, 15 965–15 971, 2016.

[183] Fedotova, A., M. Younesi, J. Sautter, A. Vaskin, F. J. F. Löchner, M. Steinert, R. Geiss, T. Pertsch, I. Staude, and F. Setzpfandt, "Second-harmonic generation in resonant nonlinear metasurfaces based on lithium niobate," *Nano Letters*, Vol. 20, No. 12, 8608–8614, 2020.

[184] Yuan, S., Y. Wu, Z. Dang, C. Zeng, X. Qi, G. Guo, X. Ren, and J. Xia, "Strongly enhanced second harmonic generation in a thin film lithium niobate heterostructure cavity," *Physical Review Letters*, Vol. 127, No. 15, 153901, 2021.

[185] Tu, X., S. Feng, J. Li, Y. Xing, F. Wu, T. Liu, and S. Xiao, "Enhanced second-harmonic generation in high-Q all-dielectric metasurfaces with backward frequency conversion," *Physical Review A*, Vol. 109, No. 6, 063522, 2024.

[186] Hu, B., X. Yang, J. Wu, S. Lu, H. Yang, Z. Long, L. He, X. Luo, K. Tian, W. Wang, *et al.*, "Highly efficient octave-spanning long-wavelength infrared generation with a 74% quantum efficiency in a $\chi^{(2)}$ waveguide," *Nature Communications*, Vol. 14, No. 1, 7125, 2023.